ANTERIOR TEETH ROOT MORPHOLOGY PREDICTION AS DERIVED FROM DIGITAL MODELS: A COMPARATIVE STUDY OF PLASTER STUDY CASTS AND NATURAL TEETH FROM DRY SKULLS

By

Panagiota Magkavali-Trikka
D.D.S., Aristotle University of Thessaloniki, 2013

Presented to the Hamdan Bin Mohammed College of Dental Medicine of
Mohammed Bin Rashid University of Medicine and Health Sciences
in Partial Fulfillment of the Requirements for the Degree of
Master of Science in Orthodontics

2018

ABSTRACT

Anterior teeth root morphology prediction as derived from digital models:

A comparative study of plaster study casts and natural teeth from dry skulls

Panagiota Magkavali-Trikka, D.D.S.

Supervisors:

Professor Athanasios E. Athanasiou

Professor Demetrios J. Halazonetis

Aim:

To assess the accuracy and reliability of the digital images of dental models generated by specific commercially available software in predicting root morphology characteristics in comparison to the corresponding natural teeth.

Materials and Methods:

The initial sample of 56 natural teeth derived from14 dry human skulls with permanent dentition. From the 14 dry skulls, there were 11 mandibles and 3 maxillae. The inclusion criteria used in this study were that all the teeth should derive from permanent dentition of adults and should present normal crown morphology. Primary teeth, teeth with abnormal tooth morphology and restorations, and jaws resembling craniofacial anomalies or syndromes were excluded. Based on these criteria, one maxillary right lateral incisor was excluded since it had a fractured crown. Therefore, the total number of the sample of teeth used was 55. The sample size calculation required 43 teeth. Upper and lower dental arch impressions, utilizing alginate material, were taken and plaster study models were fabricated. The maxillary and mandibular plaster models were

scanned using the Ortho Insight 3D laser scanner. Using the Ortho Insight 3D software (version 4.0.6), measurements, to the nearest 0.01 mm, were recorded by locating relevant landmarks using the intrinsic linear measurement function of the software. Based on these landmarks, the software produced virtual roots for the selected teeth. Then both the scanned casts and their root predictions were exported in stereo-lithography (STL) files. All corresponding 55 natural teeth were removed from the upper and lower jaws of the dry skulls and scanned using the Identica extraoral white-light scanner in order to calculate their actual root morphological characteristics. In order to acquire the whole tooth geometry, the teeth were scanned twice, once to acquire the crown and the cervical part of the root, and a second time to acquire the remaining part of the root, including the apex. The two scanned segments were joined in software by superimposing them along their common part. Finally, the accuracy of the digital models generated by the Ortho Insight 3D laser scanner in predicting root morphology characteristics was assessed by comparing these results to the corresponding measurements of the 55 natural teeth. The long axes of the tooth models obtained from the software prediction and the scanning of the actual teeth were computed and the discrepancy between them evaluated.

Results:

The error of the method was evaluated by repeating the measurements on 14 teeth. The differences in root mean squared error (RMSE) of superimposition of the two scanned segments (crown - root) of each tooth ranged from -0.006 to 0.010 mm. The differences in RMSE of superimposition of each tooth on its corresponding cast ranged from -0.040 to 0.057 mm. Both these error ranges showed acceptable accuracy. The error in calculating the angulation between the predicted and actual long axes ranged from -3.2 to 2.3 degrees (95% limits of agreement: -3.7 to 3.2).

The predicted tooth angulation was found to differ significantly from the actual angulation, both statistically and clinically. The angle between the predicted and actual long axes ranged from 2.0 to 37.6 degrees (average: 9.7 degrees; median: 7.4 degrees).

Conclusions:

Based on the results of this study, the degree of error is higher for mandibular central incisors and maxillary lateral incisors, and lower for maxillary central incisors and mandibular lateral incisors. Further investigations and improvements of the software are needed before it can be considered clinically effective.

DEDICATION

The work of my Master Thesis is dedicated to the following:

To *my beloved mother*, who has a major contribution in what I have achieved until today. Her motivation and unconditional love gave me courage to make the completion of this work possible.

To *my dearest father*, without his support, encouragement and eternal care, I would never be able to implement all my ambitions.

To *my cherished sister*, who is a source of hope for me. I am thankful for having her always by my side.

To *my family, friends* and *colleagues*, I am grateful to have them in my life.

DECLARATION

I declare that the entire content of the thesis is my own work. There is no conflict of interest with any other entity or organization.

Name: Panagiota Magkavali-Trikka

Signature:

ACKNOWLEDGMENTS

This study was conducted with the kind guidance of supervisors, professors and academic assistants.

I am profoundly appreciative to my mentor in the field of Orthodontics, Professor Athanasios E. Athanasiou, for the continuous motivation, invaluable assistance and insightful comments in the course of this project. He has always been encouraging and provided fruitful guidance.

I would like to express my sincere gratitude to Professor Demetrios J. Halazonetis for his intellectual support, devotion and for facilitating a great part of my project through his software design. He inducted me into the methodology of this project and provided indispensable information in order to enrich my understanding.

I am grateful to the Assistant Professor Eleftherios G. Kaklamanos for his great support which led me to overcome the challenges of this study.

I am thankful to Mr. Evangelos Sotiropoulos, Senior Orthodontic Technician, for his contribution with his knowledge.

List of Tables

Table 1. A brief summary of existing differences between the characteristics of plaster and digital models (Peluso et al., 2004).

Table 2. Number and classification of the teeth of the study's sample.

Table 3. Representation of the encoding system used for the sample of the teeth.

Table 4. Landmarks of teeth to be detected by operator on Motion View software.

Table 5. Analytic representation of the teeth's angles.

List of Figures

Figure 1. Mathematical model of a cone and a truncated cone used for the calculation ofthe root surface area (redrawn from Melsenet al., 1989).

Figure 2. Scanned plaster model, imported to the Ortho Insight Software (082) (Courtesy of Motion View Software LLC; printed with permission).

Figure 3. Digitizing the model and separating the teeth (Courtesy of Motion View Software LLC; printed with permission).

Figure 4. Detection of landmarks (Courtesy of Motion View Software LLC; printed with permission).

Figure 5.Setting of the facial axes (Courtesy of Motion View Software LLC; printed with permission).

Figure 6. Root prediction and alignment of the roots with their corresponding crowns (Courtesy of Motion View Software LLC; printed with permission).

Figure 7. Exported roots' predictions in STL file (Courtesy of Motion View Software LLC; printed with permission).

Figure 8. A unified tooth after the first superimposition of crown and root.

Figure 9.A superimposition of the tooth with the scanned plaster model.

Figure 10. A superimposition of the scanned plaster cast and the Ortho Insight prediction.

Figure 11. Estimation of the angulation between the long axes of the roots after the superimposition of the crown of the tooth with the crown of the prediction derived from the Ortho Insight Software.

Figure 12. Tooth-Root Bland Altman Plot.

Figure 13. Tooth-Cast Bland Altman Plot.

Figure 14. Superimpositions between tooth-root, tooth-cast and cast-prediction.

Figure 15. The error of the method for the difference in angulation between the real teeth and their predictions.

Figure 16. Difference in angulation between the real scanned teeth and their predictions.

Figure 17. Detailed graph indicating the difference in the angulation of the real teeth and their corresponding predictions per tooth.

Figure 18. Normality test to assess the distribution of the teeth angles.

Table of Contents

Pages

GENERAL SECTION .....**Σφάλμα! Δεν έχει οριστεί σελιδοδείκτης.**

1. Introduction 1

2. Literature review 3

2.1. Anterior Permanent Teeth Anatomy 4

2.1.1. Crown of the Permanent Maxillary Central Incisors 5

2.1.2. Crown of the Permanent Maxillary Lateral Incisors.....6

2.1.3. Root of Permanent Maxillary Incisors 7

2.1.4. Crown of Permanent Maxillary Canines.....8

2.1.5. Root of Permanent Maxillary Canines.....9

2.1.6. Crown of Permanent Mandibular Incisors 9

2.1.7. Root of Permanent Mandibular Incisors 10

2.1.8. Crown of Permanent Mandibular Canines.....11

2.1.9. Root of Permanent Mandibular Canines 11

2.2. Methods of Root Morphology Assessment.....12

2.2.1. Intraoral Periapical Radiographs.....13

2.2.2. Panoramic Radiographs 15

2.2.3. Cone Beam Computed Tomography.....18

2.2.4. Magnetic Resonance Imaging 21

2.2.5. Mathematical Models.....23

2.2.6. Prediction Derived from Digital Models.....24

2.3. Digital Dental Models 26

2.3.1. Extraoral Scanners 26

2.3.2. Intraoral Scanners.....27

2.3.3. Combined Scanning and 3D Maxillofacial Imaging.....29

2.3.4. Root Morphology Assessment from Digital Models 30

SPECIAL SECTION ..... **Σφάλμα! Δεν έχει οριστεί σελιδοδείκτης.**

3. Research Hypotheses 31

4. Aim 32

5. Materials and Methods 33

5.1. Materials 33

5.2. Methods 37

6. Statistics 47

6.1. Sample Size Calculation 47

6.2. Statistical Methods 48

6.3. Method Error 48

7. Results 50

8. Discussion 59

9. Conclusions 63

10. References 64

1. Introduction

Successful orthodontic treatment primarily rests on comprehensive diagnosis and methodical treatment planning. One of the most widely used and reliable diagnostic tools in orthodontics for classifying malocclusions, identifying aberrations and formulating treatment objectives comprise plaster study models (Stewart, 2001). These are presented as the "gold standard" as they form a dimensionally accurate representation of the occlusion (Rheude et al., 2005).

Digital models making use of advances in computer technology appeared in clinical practice in the late 1990s and their use has continued to grow since then (Fleming et al., 2011). Nowadays, the gypsum-based models commonly used in Orthodontics can be replaced by a revolutionary system of digital casts enabling the clinician to make a static analysis of all the parameters formerly considered on plaster casts (Garino and Garino, 2003). With the aid of three dimensional (3D) digital model scanning, the physical plaster model, or even the impression it derives from, are scanned by a laser scanner and reconstructed as a digital file (Leifert et al., 2009).

This excellent way of replicating the dentition into virtual images, aside from the advantage of being able to access data immediately, provides a facility of examining and analyzing digitally any existing plaster model.

In addition, such a method has the advantage of transferring and recording accurately the captured digital images along with the potential to reduce substantially the burden of model storage as well as the added benefit of being able to present the patient with the treatment plan in a more appealing way on today's high-definition computer screens (Keating et al., 2008; Akyalcin et al., 2013). (Table 1).

Table 1. A brief summary of existing differences between the characteristics of plaster and digital models (Peluso et al., 2004).

	Plaster Models	**Digital Models**
Cost	Less expensive	More expensive
Diagnostic setups	Laboratory procedure	Virtual on computer
Storage space	Large space required	Negligible
Storage costs	Costly	Negligible
Fast and efficient retrieval	Yes	Yes
Retrieval at multiple location	No	Yes
Subject to physical damage	Yes	No
Transfer of models	Laboratory duplication and shipping	Transfer of digital file
Integration with office management software	No	Yes
Patient education	Yes	Yes

Digital models, although capable of providing very accurate representations of the occlusal anatomy, suffer from a similar limitation to plaster models in that they have the limitation of showing only the crown and occlusal surfaces of the teeth, without representing the true size, location, or relationships of their roots.

A commercially available 3D laser scanner employs a diagnosis and treatment planning software that automatically calculates measurements and can provide a variety of simulations including the depiction of the roots of teeth. Root length, morphology and angulation are predicted based on information obtained from the scanned crowns of the teeth using some mathematical models.

Thus, it is very important to investigate the accuracy of these root morphology predictions when compared with the actual size and characteristics of real teeth.

2. Literature review

Plaster study models constitute a basic diagnostic record for orthodontic diagnosis, treatment planning and treatment outcome assessment. By using plaster study models, a number of measurements and analyses (e.g., tooth size vs. arch length discrepancies, tooth size discrepancies (Bolton analysis), prediction of permanent tooth size, diagnostic set-ups) can be made, which are easily reproducible and inexpensive (Peluso et al., 2004). Their importance and sufficiency as a diagnostic tool was highlighted by Han and co-workers (1991), who showed that the availability of a full set of diagnostic records; that is study models, photographs, panoramic x-rays, and lateral cephalometric radiographic tracings, had minimal effect on the treatment decision compared to using study models alone.

In addition to these useful characteristics of plaster study models, some limitations are inherent to their nature. They are fragile and fracture easily, making it desirable for orthodontists to keep duplicates, which is a costly and time-consuming process (Akyalcin, 2011). Over time, their continued use for measurements and display can wear away plaster and decrease their accuracy as a diagnostic tool. Their portability and the sharing of information become difficult when only one set of plaster models exists, not to mention the long-term storage that is required from the beginning until the end of orthodontic treatment (Peluso et al., 2004).

Introduction of digital models in orthodontics presented a significant number of advantages in comparison to the traditional plaster study models. The accuracy of digital models has been tested for both diagnosis and the implementation of the treatment plan in orthodontic patients. Rheude and co-workers (2005), investigated the diagnostic and treatment planning value of digital models in comparison with plaster study casts and found that the degree of recorded changes in the measurements made was minor and considered to be clinically insignificant. A more recent study confirms that digital

models are as reliable as traditional plaster models, exhibiting high accuracy, reliability, and reproducibility. Furthermore, given their advantages in terms of cost, time, and space required, a case can be made for considering them the new gold standard in current practice (Rossini et al., 2016). Last but not least, there is evidence that the digital models can facilitate precise and accurate measurements, as well as visualizations of the proposed treatment outcomes (Peluso et al., 2004).

Evolution in relevant software capabilities has been able to produce digital models which do not only include the clinically visible part of the dental arch but also facilitate images that resemble prediction of the roots of the teeth (Dastoori, 2016).

2.1. Anterior Permanent Teeth Anatomy

The nature of human dentition has been continuously changing in form, size and number over time. The general trend is towards a simplification of the morphology of the 32 teeth found in early humans. According to Koussoulakou and co-workers (2009), human teeth originate from a common precursor and develop under similar molecular instruction, while the morphological differences between the individual teeth in a dentition arise mainly from the spatiotemporal expression of certain odontogenic genes. These genes, encode transcription factors that regulate other signaling factors, which in turn mediate interactions between the odontogenic tissue layers and affect cell multiplication, cyto-differentiation and cell death (Thesleff et al., 1995; Matalova et al., 2008).

All teeth, including the anterior permanent ones, have two distinct parts: the crown, which is located above the neck and is visible in the oral cavity, and the root which supports a straight neck surrounded by a band of gingival tissue (Liebgott, 2001).

Regarding their histology, teeth are composed of four specific types of tissues namely enamel, cementum, dentine and the pulp chamber. Enamel is a very hard tissue that covers the dentine of the crown of the tooth and consists of tightly packed calcified

prisms. The cementum comprises a thin layer of a bonelike substance covering the root surface and connected to the collagenous fibers of the periodontal ligament. The dentine comprises the structural body of the pulpal cavity and the root canal, whereas the pulp chamber contains all pulpal soft tissues, such as odontoblasts, connective tissue cells, blood vessels and nerves. The pulp chamber extends to the apical foramen, from which alveolar vessels and nerves enter or leave the tooth substance (Liebgott, 2001).

As per the part of the dental descriptive anatomy, both the crown and root morphology of the upper and lower anterior teeth will be addressed in detail in the following section.

2.1.1. Crown of the Permanent Maxillary Central Incisors

The permanent maxillary central incisors are situated in the anterior part of the dental arch, close to the median line, with their mesial surfaces being in contact with each other (Black, 1902). They are considered to be the widest teeth among all anterior units with regards to their mesiodistal part (Scheid and Weiss, 2017). Their crown is "wedge shaped" with rounded angles and significantly longer inciso-gingivally than mesiodistally (Scheid and Weiss, 2017). Regarding their labial surface, it can be described as convex, although in certain cases it can be flattened in both the middle and incisal parts (Nelson and Ash, 2010; Scott and Symons, 1977). In cases of a newly erupted tooth, mamelons are commonly seen on the incisal ridge (Nelson and Ash, 2010; Scott and Symons, 1977). The lingual outline has the form resembling the letter S and it is convex at the area of the cingulum, while being concave or almost flat from the cingulum to the incisal edge. Its surface is roughly triangular and surrounded by marginal ridges, which run from the incisive edge to the cingulum plateau and are less prominent in the lingual half, as they converge at that point (Scheid and Weiss, 2017; Scott and Symons, 1977). Cases of shovel-shaped maxillary central incisors, in which an exaggeration of the marginal ridges is described, can also be found in some ethnic groups such as Asians and Native Americans as an effect of non syndromic variations in

the EDAR gene (Nelson and Ash, 2010) (Kimura et al., 2009). A lingual fossa is located between these marginal ridges and incisally to the cingulum. It is usually smooth, but in certain cases it can appear as a deep pit at the junction of the gingival ridge with the lingual surface (Scheid and Weiss, 2017). The mesial and distal surfaces are described as having the outline of a letter V and are both lingually inclined (Scott and Symons, 1977). More specifically, the mesial surface is relatively flat from the angle of the cutting edge to the gingival line, whereas the distal one is slightly more convex. Their mesial margin is also slightly longer and straighter than the distal one. The angle formed by the incisal edge and the mesial surface is approximately a right angle, while that formed by the distal surface and the incisive edge is also more rounded similarly to the distal proximal side (Scott and Symons, 1977).

2.1.2. Crown of the Permanent Maxillary Lateral Incisors

The permanent maxillary lateral incisors supplement the central ones in function and esthetics. Their crowns exhibit similar morphology, with the lateral incisors having smaller dimensions with the exception of the length of the root (Scott and Symons, 1977; Nelson and Ash, 2010). The two main differences to the maxillary central incisors is that the laterals present a more rounded angle in the incisive edge with the distal surface and in front of the cingulum plateau there is a well-marked fossa or pit (Scott and Symons, 1977). More specifically, the labial surface of the crown is more convex in the mesiodistal direction, with the exception of some square or flat-shaped forms, the mesial angle is steep, and the incisal edge terminates in a rounded and obtuse angle (Nelson and Ash, 2010; Black, 1902). As far as its concavity is concerned, the lingual surface of the maxillary lateral incisor is quite uneven. Some can be flat, whereas others are deeply concave and it is not uncommon to find a deep developmental groove at the side of the cingulum, usually on the distal side, which can even extend to the root of the tooth. The proximal surfaces present the V-shaped characteristics similar to the

maxillary central incisors. The mesial surface is rounded close to the incisal edge labiolingualy, but is much more flattened close to the gingival line. It should also be mentioned that the distal aspect appears slightly thicker than the mesial one from the marginal ridge to the labial aspect (Nelson and Ash, 2010).

2.1.3. Root of Permanent Maxillary Incisors

The roots of both permanent maxillary incisors present comparable characteristics, as they are single-rooted, conical in form and wide faciolingually at the cervix, while they taper towards a relatively blunt apex (Scott and Symons, 1977;Scheid and Weiss, 2017; Nelson and Ash, 2010). The length of the root of maxillary central incisors is about one and a fourth to one and a half times when compared to the height of the crown to the cervix, while the length of the root of the maxillary lateral incisor is approximately just one and a halftimes when the same comparison is made.

The lingual root outline for both of them is almost straight in the cervical third and gradually curves labially toward the tip in the middle and apical thirds, while the labial one is more straight. The flatter buccal root outline and the more convex lingual root outline represent a very common characteristic of these teeth when observed from the proximal view (Scheid and Weiss, 2017). In addition, these two outlines converge at the lingual aspect, giving to the root a form of a prism with fairly rounded angles.

It is important to mention two characteristics regarding the root of the maxillary lateral incisor. Firstly, it tapers more evenly than the root of a central incisor toward the blunt apex. Secondly, in most cases, it curves sharply from this location in a distal direction and ends in a pointed apex, although some roots might appear straight, while others might appear to be curving mesially (Nelson and Ash, 2010).

The mesial root surfaces of both types of maxillary incisors can have a slight depression in the middle third cervicoapically, slightly lingual to the center faciolingually, but the distal root surfaces are likely to be convex (Scheid and Weiss, 2017).

2.1.4. Crown of Permanent Maxillary Canines

The permanent maxillary canines are positioned behind the incisors and in front of the premolars. They possess large and strong roots compared to the rest of the teeth OR to the rest of the dentition, without displaying their crowns to an excessive degree beyond the level of the adjacent teeth (Scott and Symons, 1977). They take their name from the single and prominent cusp of their crown (Black, 1902).

From a labial aspect, the mesial half of the crown is comparable to a portion of an incisor, whereas the distal half resembles a portion of a premolar. The labial surface of the canine has a greater convexity mesiodistally, characterized by a strongly marked ridge. Similar to the incisors, the facial side of any canine crown is formed by three labial lobes.. The middle lobe forms the labial ridge, which can be quite prominent and runs across the crown at the middle and incisal ends. Moreover, shallow depressions may be evident mesially and distally to the labial ridge (Nelson and Ash, 2010). The cusp tip and cusp ridges of the maxillary canine make up nearly 1/3 of the cervicoincisal length of the crown, because the angle formed by the cusp ridges is relatively sharp. Their lingual anatomy has similar characteristics to the labial one, but is noticeably narrower toward the gingival line. These teeth possess a prominent lingual ridge running cervicoincisally from the cusp to the cingulum and dividing the lingual surface into two shallow fossae. The marginal ridges are raised from the mesial and distal angles and connected to the gingival ridge or cingulum. The cingulum and the tip of the cusp are usually centered mesiodistally. On the proximal surfaces the wedge or triangular-shaped crown with a massive cusp formed by the prominent labial and lingual ridges can be observed. More specifically, the mesial surface is usually convex in all directions, but becomes flat or slightly concave near the gingival line. The distal surface exhibits more convexity compared to the mesial one and gradually becomes even more convex close to the gingival line (Scheid and Weiss, 2017).

2.1.5. Root of Permanent Maxillary Canines

The root of the permanent maxillary canine is usually longer than any other root in the dentition, averaging 17.5 mm and ranging from 11 to 21 mm. Its shape is irregularly conical in form, tapering from the neck to the apex and its labiolingual diameter is greater than its mesiodistal (Black, 1902). In general form, it is thick labiolingually, with developmental depressions mesially and distally, while its surface appears smooth from the labial aspect (Nelson and Ash, 2010). The root contours are usually convex lingually and narrower mesiodistally on the lingual half than on the labial half. In this way, it is often possible to see both mesial and distal sides of the root and one or both longitudinal depressions from this aspect. In addition, the roots often have longitudinal depressions on the mesial and distal surfaces, with the distal ones being more prominent. The apical third is narrow mesiodistally and the apex can be pointed or sharp (Scheid and Weiss, 2017).

2.1.6. Crown of Permanent Mandibular Incisors

All permanent mandibular incisor crowns are relatively narrow in relation to their crown length. The mandibular central incisor, however, has the narrowest crown of all the teeth in the mouth, but its shape is so symmetrical that it is usually difficult to differentiate the left from the right tooth. The only noticeable difference between them is the greater mesial than distal curvature of the cervical line (Nelson and Ash, 2010). Regarding the shape of the mandibular lateral incisor, this is comparable to that of the mandibular central incisor, but slightly wider and not bilaterally symmetrical. The crown usually seems to tilt distally on its root, which makes the curved distal outline of the crown appear shorter than the mesial one (Scheid and Weiss, 2017).

The labial surfaces of both central and lateral incisors are smooth, with two shallow developmental depressions in the incisal third. More specifically, the labial aspect of the mandibular central incisor tapers evenly from the relatively sharp mesial and distal incisal angles to the apical portion of the root. The incisal ridge of the crown is straight

and at 90 degrees to its longitudinal axis. The mesial and distal sides of the crown taper evenly from the contact areas to the narrow cervix. Similar characteristics apply to the labial surface of the lateral incisor, with the difference that there is sometimes an extra 1 mm of crown mesiodistally on the distal half. The lingual surface of the crown is smooth, with a very slight concavity at the incisal third between the inconspicuous marginal ridges. Occasionally, the marginal ridges are more apparent near the incisal edges rendering the concavity between them more prominent as a result. From the lingual aspect, both of them present a cingulum plateau; the one of the central incisors is convex, small and centered on the axis of the root, whereas that of the lateral incisor lies slightly distal to the axis of the root (Nelson and Ash, 2010). The lingual fossa of both incisors are barely visible, smooth and shallow and just slightly concave in the middle and incisal thirds. Finally, the marginal ridges of the mandibular incisors are often scarcely discernible and it is worth noting that the mesial marginal ridge on these teeth appears longer than the distal one. As per the proximal views, the labial crests of curvature on both types of mandibular incisors are in the cervical third, where the labial outlines become nearly flat in the incisal thirds and the lingual outlines are “S” shaped, as also seen in the cervical third on the cingulum (Scheid and Weiss, 2017).

2.1.7. Root of Permanent Mandibular Incisors

The roots of both types of permanent mandibular incisors appear very narrow mesiodistally, but wide faciolingually, and taper uniformly on both sides from the cervical line to the apex. In addition, the apical end may curve slightly to the distal in some cases (Scheid and Weiss, 2017).

They are slender, relatively flattened in their mesiodistal diameter and usually grooved on the mesial and distal sides (Black, 1902). As for the lingual surfaces, these are mostly convex and slightly narrower on the lingual side than on the labial side for both teeth. From the proximal sides, it can be seen that the facial and lingual outlines of the roots

are almost straight from the cervical line to the middle third after which the root tapers with its apex on the midroot axis line. There is also a slight longitudinal depression on the middle third of the mesial and distal root surfaces of both mandibular incisors. The distal depressions are slightly more distinct (Scheid and Weiss, 2017).

2.1.8. Crown of Permanent Mandibular Canines

Permanent mandibular and maxillary canines bear a close resemblance to each other. The crown of the mandibular canine is narrower mesiodistally than that of the maxillary and can be 0.5 to 1 mm longer. The labial surface of the mandibular canine is smoother and more convex than that of the upper. Its crown appears longer and narrower and the ridges on the cusp form a more obtuse angle than the corresponding angle on the maxillary incisor (Black, 1902). From the lingual side, the marginal ridges, together with the lingual ridge and fossae, are often inconspicuous, and the cingulum is low, less massive and prominent than is the case with maxillary incisors. The lingual surface of the crown is smoother and less pointed towards the marginal ridges. The cusp of the mandibular canine is not as well-developed as in the maxillary canine and the cusp ridges are narrower labiolingually. Usually the cusp tip is in line with the center of the root, from the mesial or distal aspect, but sometimes it lies lingual to the line compared to the mandibular incisors. The proximal sides are also wedge shaped, but they are thinner in the incisal portion than the maxillary canines, because of a less bulky lingual ridge(Nelson and Ash, 2010; Scott and Symons, 1977).

2.1.9. Root of Permanent Mandibular Canines

The roots of permanent mandibular canines are shorter than those of maxillary canines, and they taper apically to a blunter apex that is more often straight rather than curving toward the mesial or distal. The labial outline of the roots is often convex with the lingual outline usually more than the labial one. They have vertical depressions on the mesial and distal surfaces, with the distal ones being usually more distinct and evident

when compared to the mesial and deeper distal surfaces of the mandibular canine roots (Black, 1902). Lingually, they are convex and narrower mesiodistally in the lingual half, making it possible to see both mesial and distal sides of the root and one or both of the proximal longitudinal root depressions from this view. They taper apically to a slightly blunter apex, more frequently straight rather than curving toward the mesial or the distal (Scheid and Weiss, 2017). As for the proximal sides, they are often slightly convex with the lingual outline more convex, although this is variable. There are also vertical longitudinal depressions on the mesial and distal surfaces, with the distal being more distinct. The developmental depression mesially on the root of the mandibular canine is more pronounced and sometimes quite deep (Nelson and Ash, 2010).

A conspicuous, but rare, variation of the canine root is for it to be divided into labial and lingual roots. These roots may be split only in the apical third or the split may extend even into the cervical third of the root (Scheid and Weiss, 2017).

2.2. Methods of Root Morphology Assessment

Clinical examination and dental radiographs are vital components of thorough patient care and make a crucial contribution to accurate and comprehensive treatment planning. They help the clinician to identify many conditions, including pathological lesions and various other features of the teeth and bone. In more detail, the information that can be collected from these radiographs can include the following:

- missing or supernumerary teeth,
- impacted teeth,
- dental caries
- periodontal disease in various stages,
- tooth abnormalities,
- retained roots,
- cysts and tumors,

- identification of root morphology and their parallelism in the jaws.

The most common types and techniques of dental radiographs are described in the next sections.

2.2.1. Intraoral Periapical Radiographs

Periapical radiographs depict images of the outlines, location and mesiodistal extent of the teeth and their surrounding tissues (Langland et al., 2002). They determine the presence and position of unerupted teeth, the presence or absence of apical pathology or root form. In cases of ectopically positioned canines, peripacial X-rays can form a part of a parallax technique and, in certain cases, allow assessment of the resorption of lateral incisors (Isaacson et al., 2015). Supplementary periapical views are indicated when clinical examination, the findings of a panoramic radiograph or a treatment history require further investigation. The necessity of determining the full length of the tooth and at least 2 mm of the periapical bone must be noted (Langland et al., 2002).

In descriptive radiology, there are two intraoral projections used for periapical radiography: the paralleling technique and the bisecting-angle technique; the first of these is more commonly used since it provides a less distorted view of the dentition (White and Pharoah, 2009).

Regarding the paralleling technique, there are two fundamental rules: Firstly, the film is situated in the mouth in a position parallel to the long axes of the teeth and secondly, the central section of the X-ray beam is directed perpendicularly (at right angles) to both the long axes of the teeth and the plane of the film (Langland et al., 2002). Then, the receptor should be positioned parallel to the teeth and deep in the patient's mouth. For maxillary projections, the superior border of the receptor rests at the height of the palatal vault in the midline; whereas for mandibular projections it should be used to displace the tongue posteriorly so as to allow the inferior border of the receptor to rest on the floor of the mouth on the lingual surface of the mandible. Regarding the angulation of the

generator tube, the orientation of the beam of the X-ray equipment should be set to align with the aiming cylinder. The horizontal direction of the beam primarily influences the degree of overlap for the images of the crowns at the interproximal spaces (Iannucci and Howerton, 2006).

In general, successful periapical X-rays can be taken if the following rules are followed:

The film must be placed so that it covers the particular teeth to be examined for each region of the oral cavity.

The vertical plane of the film should be placed parallel to the long axes of the teeth being radiographed.

The horizontal plane of the film must be parallel to the horizontal planes of the respective teeth.

The central focus of the X-ray beam must be directed to the center of the film to completely cover the film (Langland et al., 2002).

Nowadays, the bisecting-angle technique has been largely replaced by the paralleling technique. However, it still remains an option when the paralleling technique cannot be applied by the operator. This technique is based on Cieszynski's rule of isometry which states that two triangles are congruent when they have one complete side in common and two equal angles. The receptor is situated as close as possible to the lingual surface of the teeth, resting on the palate or the floor of the mouth. In order to achieve a successful projection, the plane of the receptor and the long axis of the teeth should make an angle with its apex at the point where the receptor is in contact with the teeth along an imaginary line. In this way, the central focus of the beam is directed at right angles to this bisector so that two triangles are formed with two equal angles and a common side. Theoretically, the images cast on the receptor are the same length as the projected object. On the other hand, if it is required to reproduce the length of each root of a multi-rooted tooth accurately, the central beam must be angled differently for each root. Another drawback is that the alveolar ridge often appears more coronally than its true position,

thus distorting the apparent height of the alveolar bone around the teeth (Iannucci and Howerton, 2006; Biggerstaff and Phillips, 1976).

The parallel technique for obtaining periapical radiographs has been used widely when investigating and quantifying the occurrence of root resorption phenomena. It is common for periapical radiographs to be considered better than panoramic films for assessing root shape and morphology. It should be noted, though, that periapical radiographs only provide a two-dimensional (2D) projection of the tooth's complex three-dimensional (3D) structure, and in this way they may obscure potentially minor local areas of root resorption (Nasiopoulos et al., 2006).

Sherrard and co-workers (2010) tested the accuracy and reliability of tooth and root measurements from periapical images compared to CBCT scans. They found that the greatest method's errors were associated with periapical measurements, whereas the smallest errors were associated with CBCT. As a conclusion, periapical measurements were less accurate than CBCT for tooth-length and root-length measurements because of difficulties with landmark identification, as a 3D point is depicted on a 2D picture.

2.2.2. Panoramic Radiographs

As indicated by the term, panoramic radiographs show a wide view of both the maxilla and mandible in a single projection. Both the receptor and the tube head rotate around the patient, producing series of individual images. When the combination of all the images has been achieved, an overall view of the maxilla and mandible is created.

The main reasons for using panoramic radiographs are to evaluate impacted teeth, tooth eruption patterns, dentoalveolar growth and development, dental trauma as well as to detect diseases, lesions and conditions of the jaws, to examine the extent of large lesions, and to assess root morphology and parallelism (Rushton and Rout, 2006).

The basic technique for panoramic radiography is accomplished by rotating a narrow beam of radiation in the horizontal plane around an invisible rotational axis that is

positioned intraorally. More specifically, the X-rays tube rotates around the patient's head in one direction, while the receptor rotates in the opposite direction. The movement of the receptor and the tube head produces an image through a process which is known as tomography. This is an imaging technique allowing the imaging of one layer, or section, of the body while blurring the images of the structures in other planes. In panoramic imaging, this image conforms to the shape of the dental arches (Paatero, 1948).

The overall assessment of the panoramic film includes the structures of the whole maxillary and mandibular dentition, the patient's inferior turbinates and their surrounding air spaces, the maxillary sinuses, the shadow of the hard palate, the mandibular body, bilateral projection of the condyles and of the hyoid bone, the ramus of the mandible and the spine where it is not superimposed on the ramus (Langland et al., 2002). Some additional applications of panoramic imaging include the examination for intraosseous pathology, such as cysts, tumors, or infections, gross evaluation of the temporomandibular joints, evaluation of position of impacted teeth, dentomaxillofacial trauma and developmental disturbances of maxillofacial skeleton (White and Pharoah, 2009).

The advantages of this technique include the increased overall representation of the dental arches and associated structures, with reduced superimposition of anatomical structures. The anatomical images produced are relatively undistorted and it comprises a simple and fast procedure, exposing the patient to a reduced amount of radiation. It also provides the information for detecting caries, periodontal disease and pulp-associated periapical changes earlier, thus minimizing the infection control procedures required (Langland et al., 2002; Rushton and Rout, 2006).

In addition to the abovementioned advantages, the most useful feature of the panoramic image is the depiction of the full dental arch. Although there are cases in which the position of the patient or the location of an ectopic tooth can displace another tooth out

of the focal plane, all the teeth are generally well depicted on the radiographic image. Furthermore, the images of the teeth should be carefully examined for several abnormalities, such as number, position and anatomy. Gross caries, periapical lesions and periodontal disease can also be evident. However, since the resolution of a panoramic radiograph is reduced in comparison with intraoral radiographs, additional intraoral radiographs may be needed to detect subtle or incipient disease.

There are some potential 'pitfalls' regarding the images derived from the panoramic radiograph. When anterior teeth appear very wide or narrow this is due to patient malpositioning during X-ray acquisition. Thus, teeth appear wider on one side than the other suggesting that the patient's sagittal plane might be rotated. Anatomically, another point to be mentioned is that the proximal surfaces of the premolar teeth often overlap, misleading the clinician regarding the interpretation of caries.

In addition, the following points should be carefully scrutinised: the orientation of the molars; the number and configuration of the roots; the relationships of the tooth components to critical anatomic structures, such as the mandibular canal, floor and posterior wall of the maxillary sinus, maxillary tuberosity and adjacent teeth; and the presence of abnormalities in the pericoronal or periradicular bone. However, since the panoramic image is of a two-dimensional nature, such findings may need additional imaging with cone-beam computed tomography (CBCT) imaging to define the precise relationships of the roots of the impacted molars to the vital structures (Rushton and Rout, 2006; Langland et al., 2002; Farman 2007).

Some of the disadvantages encountered may include (a) a less sharp image quality than intraoral projections because of the intensifying screens, (b) limitations of the focal trough as objects of interest located outside the focal trough cannot be seen, (c) certain amount of distortion, magnification and overlapping, and (d) the relative high cost of the equipment (White and Pharoah, 2009; Rushton and Rout, 2006).

Recent studies have reported that panoramic radiographs can be used for measuring tooth lengths, crown-root ratios and tooth angulations, as long as the patients are consistently positioned in the machine and a constant same magnification is used. As per the tooth length, panoramic radiographs are used to determine changes due to various reasons incluing orthodontic treatment. However, if the lower incisors are proclined their apices may move outside the focal trough of a panoramic machine and in this case the apical area would not be imaged and the tooth would appear shorter at the end of treatment. Furthermore, a proclined incisor might appear shorter if the image is foreshortened. In both cases it could be concluded that the teeth had been shortened by resorption when in fact no resorption has taken place (Armstrong et al., 2006).

Flores-Mir and co-workers (2014) concluded that panoramic reconstructions from CBCT volumes improve measurements' accuracy over conventional images by reducing several sources of magnification and distortion. On the other hand, dental measurements are still significantly different from the anatomical lengths and their use diminishes the accuracy gains achieved by 3D technology. As a result, conventional panoramic radiographs were relative inaccurate, overestimating the lengths by 29%, while CBCT by panoramic image reconstruction underestimates the lengths by 4%.

2.2.3. Cone Beam Computed Tomography

Cone beam computed tomography (CBCT) has been used in dentistry since the mid 1990s. The common uses of a CBCT include implant placement, extraction or exposure of impacted teeth, definition and localization anatomic structures, endodontic assessment, airway and sinus analysis, evaluation of the temporomandibular joints, orthodontic applications, and evaluation of pathologies (Langland et al., 2002).

The CBCT technique consists of the use of a circular or rectangular cone shaped X- rays beam with a single 360° scan where the X-rays source and a reciprocating array of detectors simultaneously move around the patient's head, which is stabilized with a head

holder. Single projection images, similar to lateral cephalometric radiographic images, are taken at specific degree intervals, which are slightly separated from one another. The series of such basis projection images is considered to represent “the projection data”, based on which certain software programs generate a 3D volumetric data set, which can be used to provide primary reconstruction images in all three orthogonal planes (axial, sagittal and coronal) (Kumar et al., 2015).

The advantages of this type of radiograph include lower radiation dose compared to traditional computed tomography (CT) procedures, short/reduced scanning time, anatomically accurate images due to the ability to eliminate the superimposition of the structures, and the ability to save and easily transport images. In addition, there is considerably less distortion of the images of soft tissues when compared to conventional CT scans (Merrett et al., 2009). Counterbalancing these advantages, the disadvantages may include patient movement and artefacts, restricted size of the field of view, which can hide signs of pathology in certain areas, cost of equipment, lack of training in the interpretation of image data on areas outside the maxilla and mandible (Radiation Protection, European Commission, 2012).

CBCT technology has become increasingly accessible, especially in dental practice. It extensively expands the fields for diagnosis and treatment possibilities for patients (Kumar et al., 2015). More specifically, it has been used in the diagnosis of maxillofacial orthodontic and orthopedic anomalies, as CBCT imaging facilitates surgical exposure and the planning of subsequent movement. Other applications include the assessment of palatal morphologic features and dimensions, tooth inclination and torque, characterization of alveolar bone for orthodontic mini-implant placement, and determining the available alveolar bone width for the safe buccolingual movement of teeth. CBCT imaging also provides adequate visualization of the TMJ, airway spaces, and soft tissue relationships (White and Pharoah, 2009; Scarfe 2008; Carter et al., 2008).

Regarding a more detailed imaging of teeth depiction, CBCT scans portray the morphology of the roots, pulp chambers and pulp canals more accurately compared to other intraoral radiographs. Furthermore, CBCT imaging is particularly useful in evaluating multirooted teeth and roots with multiple pulp canals. The number and morphology of pulp canals and their direction through the roots are evident. For multirooted teeth, reconstruction of the image volume along the long axis of each root may also be required. The individual canals are best identified on axial sections, whereas the course of the canal through the length of the root and its exit through the apex are typically assessed on coronal and sagittal sections. In addition, morphologic variations, such as root dilacerations in the buccolingual dimension are well demonstrated on CBCT examinations. Detection of normal variations of the radicular and pulpal morphology is very important to endodontic treatment planning and pre-surgical assessment of the relationship of the roots to adjacent neurovascular structures. CBCT scans also reveal the proximity of the root surface to the cortical plates of the alveolar bone and detect anatomic variations, such as fenestrations or dehiscence defects (White and Pharoah, 2009; Scarfe et al., 2012; Merrett et al., 2009; Langland et al., 2002).

CBCT imaging is a more reliable tool for detection of root morphology and small resorption areas when it is compared with conventional panoramic radiograph. When it is to be compared with the periapical X-rays, as per the root lengths, they were underestimated by an average of 2.6 mm compared to 0.3 mm underestimation in CBCT images. On the other hand, CBCT showed poor accuracy in detecting small periapical resorptions, less than 0.8 mm in diameter, and higher accuracy when the lesions were larger than 1.4 mm in diameter, whereas periapical radiographs showed poor accuracy for all simulated resorption sizes (Alamadi et al., 2017).

According to Halazonetis (2012), assuming a continual improvement in the technology takes place, CBCT will become a valuable tool for use with all our patients in the near future. For the time being, except for certain patients, replacing the conventional

cephalometric and panoramic radiographs with CBCT radiographing imaging could lead to public health hazards. Clinicians should always be very discriminating in selecting appropriate cases for such exposures. As a consequence, the use of CBCT should be restricted to cases selected after careful assessment of the relevant risks and benefits, especially concerning patients' exposure, and only where conventional 2D imaging techniques are not sufficient (Kumar et al., 2015).

2.2.4. Magnetic Resonance Imaging

Magnetic Resonance Imaging (MRI) is a non-invasive method for detecting internal structures, differentiating between soft and hard tissues and for certain aspects of functions within the body. The principle behind MRI is the use of non-ionizing radio frequency electromagnetic radiation in the presence of controlled magnetic fields, to obtain high quality cross-sectional images of the body (Niraj et al., 2016).

MRI acquisition requires placing the patient inside a large magnetic coil. This magnetic field causes the nuclei of many atoms in the body, particularly hydrogen, to align with the magnetic field. The scanner directs a radiofrequency (RF) pulse into the patient, causing some hydrogen nuclei to absorb energy (resonate). When the RF pulse is turned off, the stored energy is released from the body and detected as a signal in a separate coil in the scanner. This signal is used to construct the MRI, in essence, a map of the distribution of hydrogen (Bushberg et al., 2012; Weishaupt et al., 2008).

MRI has several advantages over other diagnostic imaging procedures. It offers the best contrast resolution of soft tissues, no ionizing radiation is involved with MRI because the region of the body imaged in MRI is controlled with the gradient coils, and direct multiplanar imaging is possible without reorienting the patient (White and Pharoah, 2009).

Because of its excellent soft tissue contrast resolution, MRI is useful in evaluating soft tissue conditions, such as the position and integrity of the disk in the temporomandibular

joint, in evaluating soft tissue disease, especially neoplasia involving the soft tissues, such as tongue, cheek, salivary glands, and neck, in determining the malignant involvement of lymph nodes and also the perineural invasion by malignant neoplasia. In cases of osteomyelitis, it may be used to visualize edematous changes in the fatty marrow together with the surrounding soft tissue. It also may be useful in identifying the location of the mandibular nerve in cases where it is not clearly seen on panoramic or CBCT images (Idiyatullin et al., 2011; Tutton and Goddard 2002).

The disadvantages of MRI include relatively long imaging times and the potential hazard imposed by the presence of ferromagnetic metals in the vicinity of the imaging magnet. This excludes the use of MRI with any patient with implanted metallic foreign objects or medical devices that consist of or contain ferromagnetic metals. Also, patients with skin artwork should be warned that their tattoos might be "at risk," during their exposure at MRI radiology. Especially, those with black pigment or any other pigments containing iron oxide. A cold compress or a cloth could be used in order to protect them and allow them to proceed with the examination (Ross and Matava, 2011). Last but not least, some patients suffer from claustrophobia when positioned in an MRI machine (Westbrook et al., 2011).

Tymofiyeva and co-workers (2013) assessed the position and shape of malformed teeth in all 3 spatial dimensions by using dental MRI. By using natural MRI contrast, the teeth, their roots and their dental pulp could be clearly delineated. Since the use of MRI is accompanied by the complete elimination of ionizing radiation and provides the advantage of a 3D morphology, it optimizes surgical treatment and increases patient's safety. In general, MRI is a safe-well-tolerated imaging method that can be used for diagnosis of dental abnormalities in children and for orthodontic treatment and surgical planning.

2.2.5. Mathematical Models

In the process of growth, most organisms tend to display increases in size and modifications in their shape. One of the first workers who tried to model these changes was D' Arcy Thomson, whose classic work was published in 1917 (Lestrel, 1989). In order to construct a mathematical model based on this procedure, a system in terms of mathematical concepts and language is required (Melsen et al., 1989).

Simple morphologies can be described by the use of a conventional metrical approach (CMA) comprising distances, angles, and ratios as a procedure for characterizing the size and shape of complex irregular forms. In cases of forms with moderate irregularities or any of the characteristic variables of various biological organisms, difficulties in description arise. To overcome this omission in CMA, mathematical models come to the fore. To construct these mathematical models several different approaches are available; some of these being a landmark or homologous-point representation; and, alternatively, outline or boundary representation (Read and Lestrel, 1986).

Homologous-points representation, which involves CMA, is calculated based on a set of homologous points or landmarks used to describe the form. A second approach uses the outline or boundary of the form. In order to be able to accurately describe the size and shape of complex morphological forms, a numerical method is required.

Obviously there must be a relationship between the analytical model and its measurement system (Lestrel, 1989).

Following the above-mentioned approach, to estimate the area of a tooth root, its shape is approximated to that of a cone. To obtain the best possible approximation, a differentiation in the apical region can be approximated to a cone, and the remaining part of the root to a truncated cone. The calculation can then be done to estimate the surface of these two geometrical structures (Melsen et al., 1989) (Figure 1).

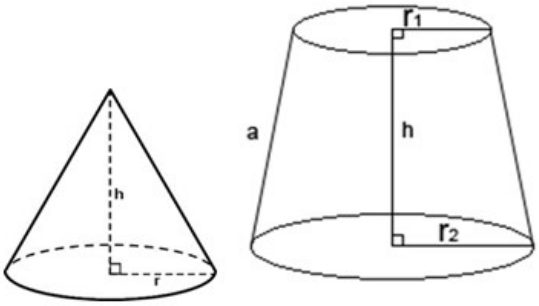

Cone:

h = height

r = radius of base

a = length of side

S = surface area

$S = \pi\, r\, a = \pi r\sqrt{r^2 + h^2}$

Truncated cone:

h = height

r_1 = radius upper base

r_2 = radius lower base

a = length of side

S = surface area

$S = \pi\,(r_1 + r_2)a =$

$\pi(r_1 + r_2)\sqrt{(r^2 - r^2)^2 + h^2}$

Figure 1. Mathematical model of a cone and a truncated cone used for the calculation of the root surface area (redrawn from Melsen et al., 1989).

2.2.6. Prediction Derived from Digital Models

There is paucity of bibliography describing tooth root prediction derived from digital dental models (Yau et al., 2014;Dastoori, 2016).

Yau and co-workers (2014) proposed a complete tooth reconstruction method by integrating 3D scanner data and computed tomography image sets. More specifically, they described a tooth reconstruction method based on the data fusion concept via integrating external scanned data and CT-based medical images. Firstly, a plaster model was digitized with a 3D scanner. Then, each crown was separated from the base according to the characteristics of the tooth. CT images were processed for feature enhancement and noise reduction, and to define the tooth axis direction which will be used for root slicing. The outline of each slice of dental root was then determined by the

levelset algorithm and converted to point cloud data. Finally, the crown and root data were registered by the iterative closest point algorithm. With this information, a complete digital dental model was reconstructed by the Delaunay-based region-growing algorithm.

Dastoori (2016) assessed the accuracy of digital models generated using commercially available software to predict anterior teeth root inclination characteristics and compared the results to relevant data obtained from CBCT images. In order to proceed with the experiment, he used pre-treatment maxillary and mandibular plaster models and the corresponding CBCT scans of patients. Randomly selected plaster models were scanned by an Ortho Insight 3D ™ scanner (Motion View Software, Chattanooga, Tennessee, USA) and CBCT scans were taken using a Kodak 9500 Cone Beam 3D System (Carestream Health, Inc., Rochester, New York, USA). The elaboration of the plaster models and CBCT data was performed according to specific technical steps. Based on the results, the maximum disparity in angle between images derived from digital models and CBCT data was almost 40 degrees (upper left canine) with the disparity in upper right canines being similar. The upper and lower canines produced the worst results, followed by the lower lateral incisors. The upper central incisors showed the best results, although the maximum angle of difference exceeded 20 degrees (with a median error only around 8 degrees). There was no statistically significant difference in measurements of difference between long axes of the root by using the two methods in each tooth according to Angle classification. It was concluded that root morphology imaging prediction is not a primary function of this software and the study confirmed its limitation as a sole tool in routine clinical applications. At present these predictions cannot be considered accurate or reliable unless correlated with a radiographic image.

2.3 Digital Dental Models

2.3.1. Extraoral Scanners

The use of plaster dental casts poses notable problems, including the possibility of deformation depending on the type of impression material, the risk of loss or damage during storage, and storage space constraints.

Extraoral scanners produce electronic models and have reached an acceptable level of accuracy. Accuracy is defined as the “closeness of agreement between a quantity value obtained by measurement and the true value of the measure” and involves trueness and precision (Mandelli et al., 2016). An example of the extraoral in-house scanner is the Ortho Insight3D® laser surface scanner with Motion View Software (Motion View Software LLC, Chattanooga, TN) (Porter et al., 2017). Since the method for digital model articulation is different depending on the specific scanner used, the extraoral Motion View scanner creates digital models in articulation by scanning maxillary and mandibular plaster casts with a physical bite registration(Porter et al., 2017).

Digital models produced with extraoral scanners have been shown to be valid when compared to direct measurement on plaster models, with the differences between the approaches considered to be clinically acceptable (Jacob et al., 2015).Apart from their accuracy, they also provide users with rapid processing and reproducibility. Since their introduction the time and cost involved in using extraoral scanners has been significantly reduced and new hardware systems and software have become available. In addition, digital models can be made from scanning the alginate impressions of the corresponding arches and show high degree of accuracy regarding intra-arch measurements. A recent systematic review by Rossini and co-workers (2016) of the diagnostic accuracy and measurement sensitivity of digital models indicated that, ingeneral, intra-arch measurements from digital casts are extremely accurate. However, it is reported that inter-arch (articulation) related characteristics such as occlusal indices, occlusal contacts, and occlusal relationships exhibited significant differences.

2.3.2. Intraoral Scanners

Intraoral scanners are presently used for producing 3D digital models (Anh et al., 2016). Chairside oral scanners allow direct digital acquisition of the intraoral situation with satisfactory accuracy, and can eliminate the need for conventional impressions (Grunheid et al., 2014). Akyalcin and co-workers (2013) confirmed that this kind of direct digital acquisition of the dental arches can provide almost 1-to-1 diagnostic information of the investigated anatomy and was superior to cone-beam computed tomography measurements.

Several types of intraoral scanners have become commercially available with 3M Oral Care (St. Paul, Minneapolis, USA), 3Shape (Copenhagen, Denmark), Align Technologies (San Jose, USA), Carestream Dental (New York, USA),and Dentsply Sirona (New York, USA) being some of th manufacturers. All of them have specific functions and possess different characteristics regarding size, weight, price, unique features and the potential for integration with other brands on the market (www.orthodontic productsonline.com).

The digitized models offer several advantages, including easy storage and the possibility of computerized data acquisition and modeling. In addition, digital impression methods employing intraoral scanners also completely eliminate the conventional impression taking process using impression materials with the added advantages of reducing the gag reflex of the patient being generally more comfortable, as breathing is freely permitted during the impression-taking process with scanners (Anh et al., 2016).

Obviously, the potential advantages of direct scanning technology would be negated if the accuracy and efficiency involved were not comparable with the conventional approach of model acquisition with alginate impressions.

Especially for orthodontics, the most important expectation from a digital model system lies in its diagnostic accuracy and reliability. Although the consensus is that measurements with digital models compare well with those derived from plaster models,

several studies investigating complex measurements, such as space available, irregularity index, and Bolton analysis indicated that mean differences between the plaster and digital models can exceed 1.5 mm. This comprises a degree of difference possibly compromising clinical acceptability (Grunheid et al., 2015).

On the other hand, there is evidence in the literature supporting the validity of digital models for the aforementioned measurements. These studies argue that digital models produced from intraoral scans can be as accurate as those from alginate impressions (Akyalcin et al., 2013). However, since impressions require less chairside time and are preferred over intraoral scans by most patients, they are currently the preferred acquisition method for digital models in conjunction with extraoral scanning. As scanning technologies evolve to become faster and more efficient, direct scanning may become more readily accepted in the orthodontic setting (Grunheid et al., 2015).

Regarding their technology, digital intraoral scanners are considered Class I medical electrical devices, designed and constructed in accordance with the standards of ANSI/IEC 60601-1. Every scanner has three major components namely (a) a wireless mobile workstation to support data entry, (b) a computer monitor to enter prescriptions, approve scans, and review digital files, and (c) a handheld camera wand to collect the scan data inside the patient's mouth. To gather surface data points, energy from either laser light or white light is projected from the wand onto an object and reflected back to a sensor or camera within the wand. Based on algorithms, tens or hundreds of thousands of measurements are taken per inch, resulting in a 3D representation of the shape of the object (Kravitz et al., 2014).

A recent report utilized a CBCT device enabling the indirect digitalization of plaster models for digital storage, diagnosis, and planning. This method also provides an acceptable level of accuracy for the manufacturing of orthodontic appliances. Direct digitalization with intraoral scanners has been demonstrated to be equally effective, although it requires more chairside time and does not result in a higher level of accuracy

than employing indirect workflow with desktop scanners. If it was possible to manufacture the appliance so as to integrate it into a completely digital workflow, intraoral scanners would be highly suitable. On the other hand, if a physical working model is required, it should be obtained conventionally and subsequently digitized (Wesseman et al., 2017).

In cases of comparison between intraoral and extraoral scanners, many differences can be found, including the need for powder use during scan with the 3M™ True Definition scanner (3M, St. Paul, USA), continuous scanning with the iTero® Element (Align Technology, San Jose, USA) and 3M™ True Definition scanner, and the prerequisite of creating a plaster model for the Ortho Insight 3D® laser surface scanner(Porter et al., 2017).

In general, both intraoral and extraoral scanners now produce accurate intra-arch measurements.

2.3.3. Combined Scanning and 3DMaxillofacial Imaging

PlanmecaProMax 3D (PlanmecaOy, Helsinki, Finland) is a CBCT product family consisting of unique all-in-one imaging units. These units have been designed to meet the strictest of requirements in maxillofacial imaging. They support three different types of 3Dimaging (CBCT, 3D face photo and 3D model scan) and are also capable of extraoral bitewing, cephalometric and digital panoramic imaging. This flexibility between 2D and 3D allows clinics to optimize their imaging procedures, and select the appropriate techniques for each case, at minimal patient dose (www.planmeca.com).

No study is available in the literature using this equipment for assessing root morphology of teeth, except for cases were the tooth canal configuration was assessed (Sinaloglu et al., 2015).

2.3.4. Root Morphology Assessment from Digital Models

By using the Ortho Insight 3D ™ high-resolution laser scanner on either plaster dental models or dental impressions in conjunction with Motion View Software, LLC (Chattanooga, Tennessee., USA) different analyses on dental arches can be made. These include measurements of dental arch dimensions, space analysis and tooth size discrepancies (Bolton analysis). After scanning models or impressions, the electronically produced images not only include the crowns of the teeth but also indicate their roots with the use of specific mathematical/geometric predictions.

Only one study exists in the literature assessing the accuracy of digital models generated by Ortho Insight 3D laser scanners in predicting root inclination characteristics by comparison to relevant data obtained from CBCT images (Dastoori, 2016). The materials used were pre-treatment maxillary and mandibular plaster models and their corresponding CBCT scans derived from 31 patients ranging in age from 12-40 years of age. The models were scanned using the high resolution of Ortho Insight 3D scanner, while the CBCT scans were made using a different type of software with the same scanner.

The results of this study showed that an average error (angle between true root position and estimated position) of 10 degrees is to be expected, but errors of more than 20 degrees were not uncommon. Visual observation of individual cases showed that the software frequently estimates angulations indicating the overlapping of adjacent roots, a clinically impossible situation in the absence of extensive root resorption or root morphology variation. The propensity for errors was higher for canines and lower for central incisors.

Since CBCT does not describe the full morphology of teeth, with special limitations regarding the apices of the roots, a more valuable comparison would utilize real teeth; but no such study exists in the literature.

3. Research Hypotheses

The hypothesis to be tested:

The hypothesis to be tested is that there are differences between predicted root morphological characteristics generated by the commercially available 3D laser scanner software and the morphology characteristics derived from the corresponding tooth material.

Null hypothesis:

The null hypothesis is that there are no differences between predicted root morphology characteristics generated by the commercially available 3D laser scanner software and the morphological characteristics derived from the corresponding tooth material.

4. Aim

The aim of this investigation was to assess the accuracy and reliability of the digital images of dental models generated by a specific commercially available software in predicting root morphology characteristics in comparison to the corresponding natural teeth.

5. Materials and Methods

5.1. Materials

The initial sample of 56 natural teeth derived from 14 dry human skulls with permanent dentition. From the 14 dry skulls, there were 11 mandibles and 3 maxillae.

The inclusion criteria used in this study were that all the teeth should derive from permanent dentition of adults and should present normal crown morphology.

Primary teeth, teeth with abnormal tooth morphology and restorations, and jaws resembling craniofacial anomalies or syndromes were excluded.

Based on these criteria, one maxillary right lateral incisor was excluded since it had a fractured crown. Therefore, the total number of the sample of teeth used was 55.

The distribution of the 55 teeth with reference to the type and jaw is presented in Table 2.

Table 2. Number and classification of the teeth of the study's sample.

	Maxillary Anterior Teeth	**Mandibular Anterior Teeth**
Right Central Incisors	2	8
Left Central Incisors	1	6
Right Lateral Incisors	1	7
Left Lateral Incisors	2	6
Right Canines	2	9
Left Canines	2	9
Total	10	45

An encoding five digit system was generated and applied for this study in order to classify the sample into different categories between maxilla, mandible and teeth.

The first two digits represent the incremental number of jaws up to the fourteenth sample.

The third digit represents the number 1 for the maxilla and the number 2 for the mandible.

The last two digits represent the total number of the anterior teeth based on the Federation Dentaire International Notation (FDI) two digit charting system.

Table 3 represents the encoding system for the teeth included in this study.

Table 3. Representation of the encoding system used for the sample of the teeth.

Jaws		**Teeth**			**Code**
Number of Jaw	**Type of Jaw**	**Central Incisors**	**Lateral Incisors**	**Canines**	
01	2			33	01233
02	2			43	02243
02	2		42		02242
02	2	41			02241
02	2		32		02232
02	2			33	02233
03	2	41			03241
03	2	31			03231
03	2		42		03242
03	2		32		03232
03	2			43	03243
03	2			33	03233
04	2	41			04241
04	2	31			04231
04	2		42		04242

04	2		32		04232
04	2			43	04243
04	2			33	04233
05	2	41			05241
05	2	31			05231
05	2		42		05242
05	2		32		05232
05	2			43	05243
05	2			33	05233
06	2	41			06241
06	2	31			06231
06	2			33	06233
06	2			43	06243
07	1		22		07122
07	1		12		07112
07	1			23	07123
07	1			13	07113
07	1	21			07121
07	1	11			07111
08	2	31			08231
08	2	41			08241
08	2		32		08232
08	2		42		08242
08	2			33	08233
08	2			43	08243
09	2		42		09242
09	2		32		09232
09	2	41			09241

09	2			33	09233
09	2			43	09243
10	2	31			10231
10	2	41			10241
10	2			43	10243
10	2		42		10242
11	2		33		11233
12	2		43		12243
13	1			13	13113
13	1			23	13123
13	1		22		13122
14	1	11			14111

Upper and lower dental arch impressions, utilizing alginate material, were taken and plaster study models were fabricated. The maxillary and mandibular plaster models of each jaw were scanned at the facilities of the Department of Orthodontics, Hamdan Bin Mohammed College of Dental Medicine, Mohammed Bin Rashid University of Medicine and Health Sciences by the author using the Ortho Insight 3D laser scanner (Motionview Software LLC, Chattanooga, Tenn., USA), with the scanning resolution set at “high”. Using the Ortho Insight 3D software (version 4.0.6), measurements, to the nearest 0.01 mm, were recorded by digitizing and separating the teeth and locating the necessary landmarks using the intrinsic linear measurement function of the software.

These landmarks were detected and were set by the author in order for the software to recognize the tooth and perform the prediction of its corresponding root. They included a total number of 8 points for incisors and 3 points for canines (Table 4).

Table 4. Landmarks of teeth to be detected by operator on Motion View software

Landmarks	Teeth
Central-Labial	Maxillary and mandibular central and lateral incisors
Central-Incisal	Maxillary and mandibular central and lateral incisors
Mesio-Labial	Maxillary and mandibular central and lateral incisors
Mesio-Incisal	Maxillary and mandibular central and lateral incisors
Disto-Labial	Maxillary and mandibular central and lateral incisors
Disto-Incisal	Maxillary and mandibular central and lateral incisors
CEJ Facial	Maxillary and mandibular central and lateral incisors and canines
CEJ Lingual	Maxillary and mandibular central and lateral incisors and canines
Cusp	Maxillary and mandibular canines

Thence, facial axes were detected and were set by the author. With the abovementioned data the software predicted the root morphology and inclination and both the scanned casts and root predictions were exported in stereo-lithography (STL) files.

All corresponding 55 natural teeth were removed from the upper and lower jaws of the dry skulls and scanned at the facilities of the Department of Orthodontics, Faculty of Dentistry, National and Kapodistrian University of Athens using an extraoral white-light scanner (Identica, Medit Co. Ltd, Seoul, Korea)in order to calculate their actual root morphological characteristics.

Finally, the accuracy of the digital models generated by the Ortho Insight 3D laser scanner in predicting root morphology characteristics was assessed by comparing these results to the corresponding measurements of the 55 natural teeth.

5.2. Methods

Measurements of the roots included 3D variables. In these images obtained from the electronic models and the natural teeth, the long axes were estimated and a comparison between the long axes of the prediction and those of the real scanned tooth took place.

Elaboration of data took place according to the following stages:

Stage 1

The plaster model of each jaw was scanned using the Ortho Insight 3D ™ laser scanner. The steps of the process were applied on all existing teeth of each cast, for the automated calculation of the program to take place. In this study only the anterior root predictions were taken into consideration only.

An example of the cast with the code number 082 shows on Figures 2-7.

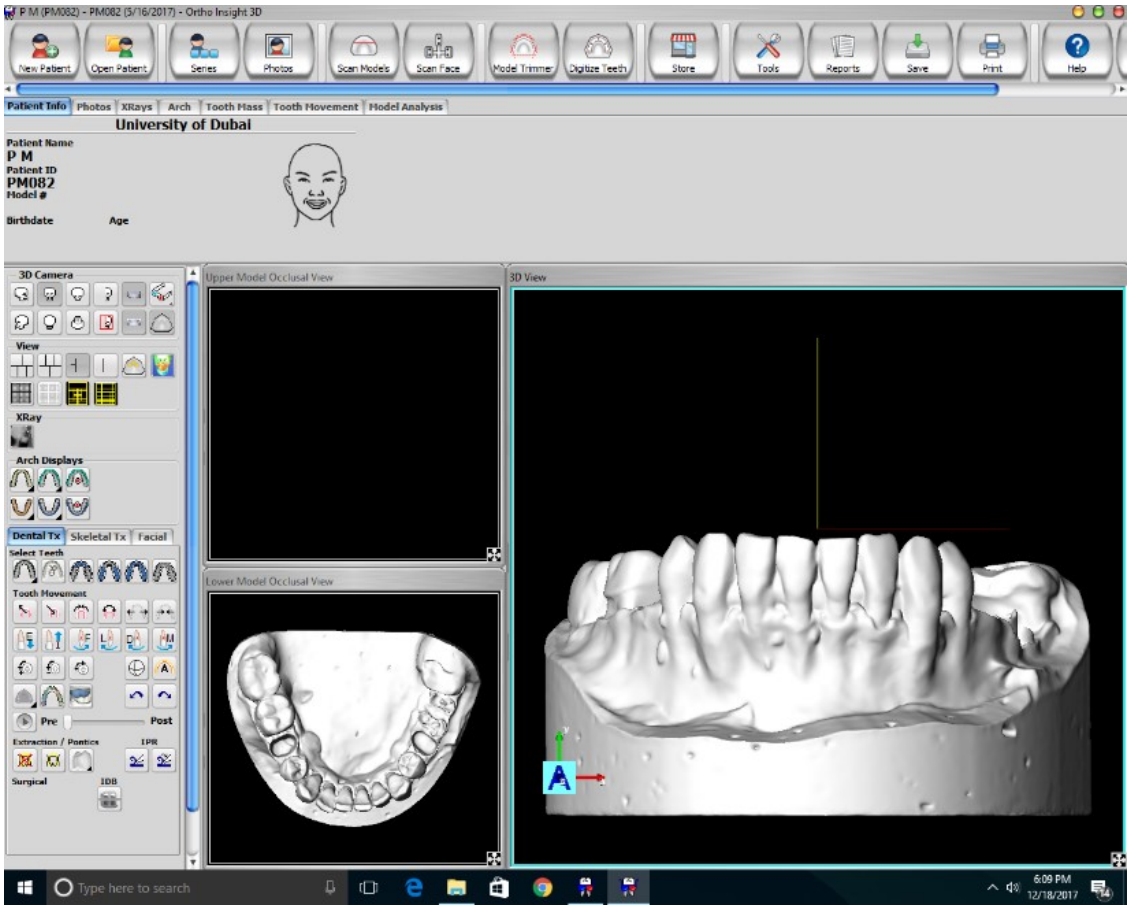

Figure 2. Scanned plaster model, imported to the Ortho Insight Software(Courtesy of Motion View Software LLC; printed with permission).

Digitizing the models started by separating the teeth (Figure 3).

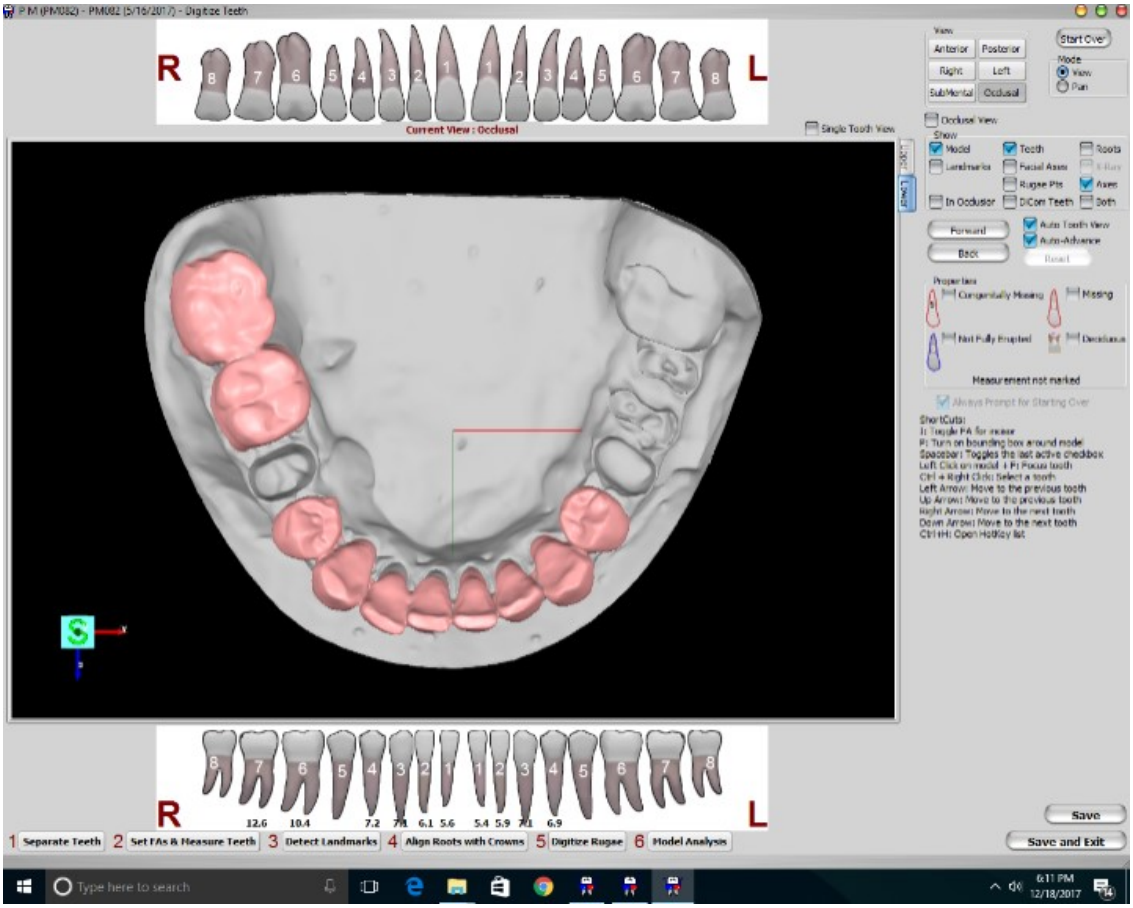

Figure 3. Digitizing the model and separating the teeth (Courtesy of Motion View Software LLC; printed with permission).

Landmarks were detected and were set by the author in order for the software to recognize the tooth and perform analysis. They included a total number of 8 points for incisors and 3 points for canines (Figure 4).

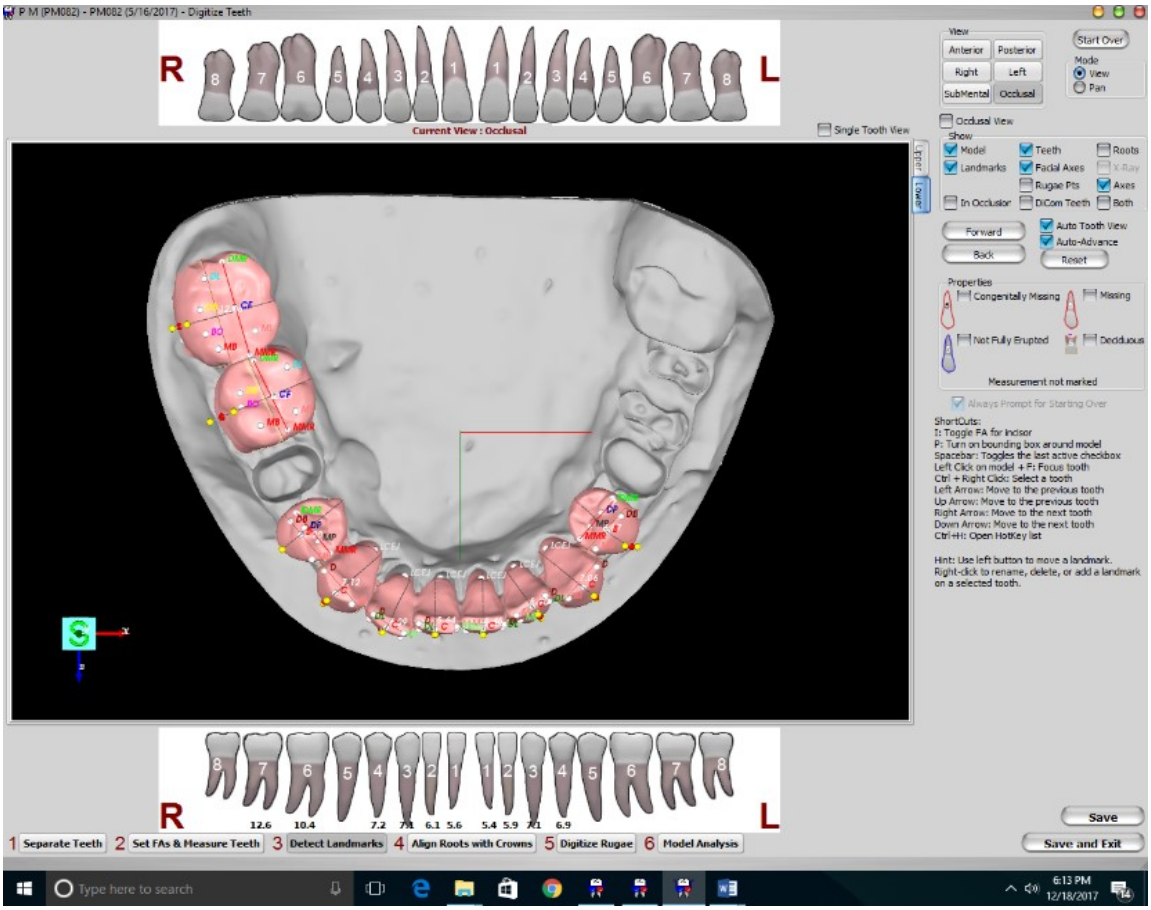

Figure 4. Detection of landmarks (Courtesy of Motion View Software LLC; printed with permission).

Facial axes were detected and were set by the author (Figure 5).

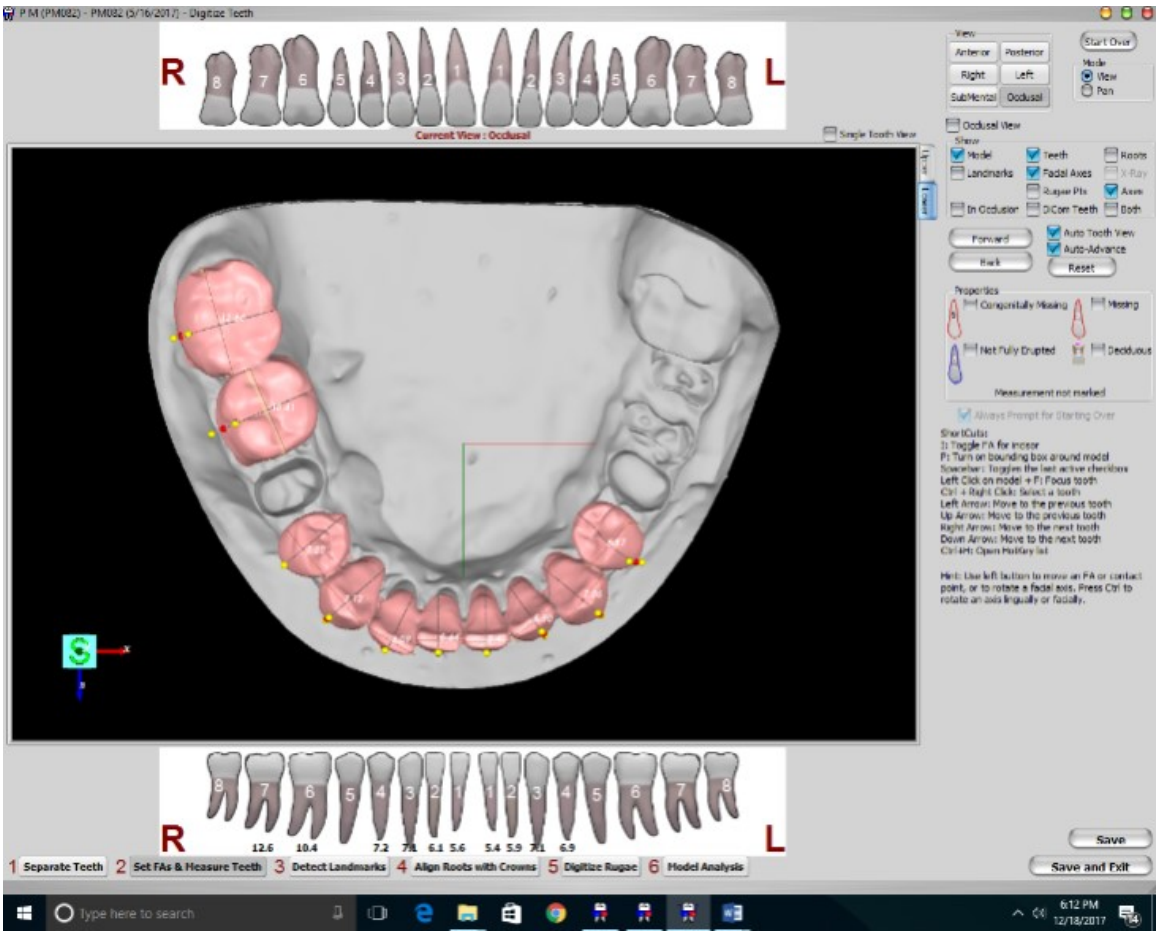

Figure 5.Setting of the facial axes (Courtesy of Motion View Software LLC; printed with permission).

During the following step, the root prediction for each tooth took place, after its alignment with the corresponding crown and models were exported to a STL file format which is readable by the Viewbox software (dHAL Software, Kifissia, Greece) (Figure 6).

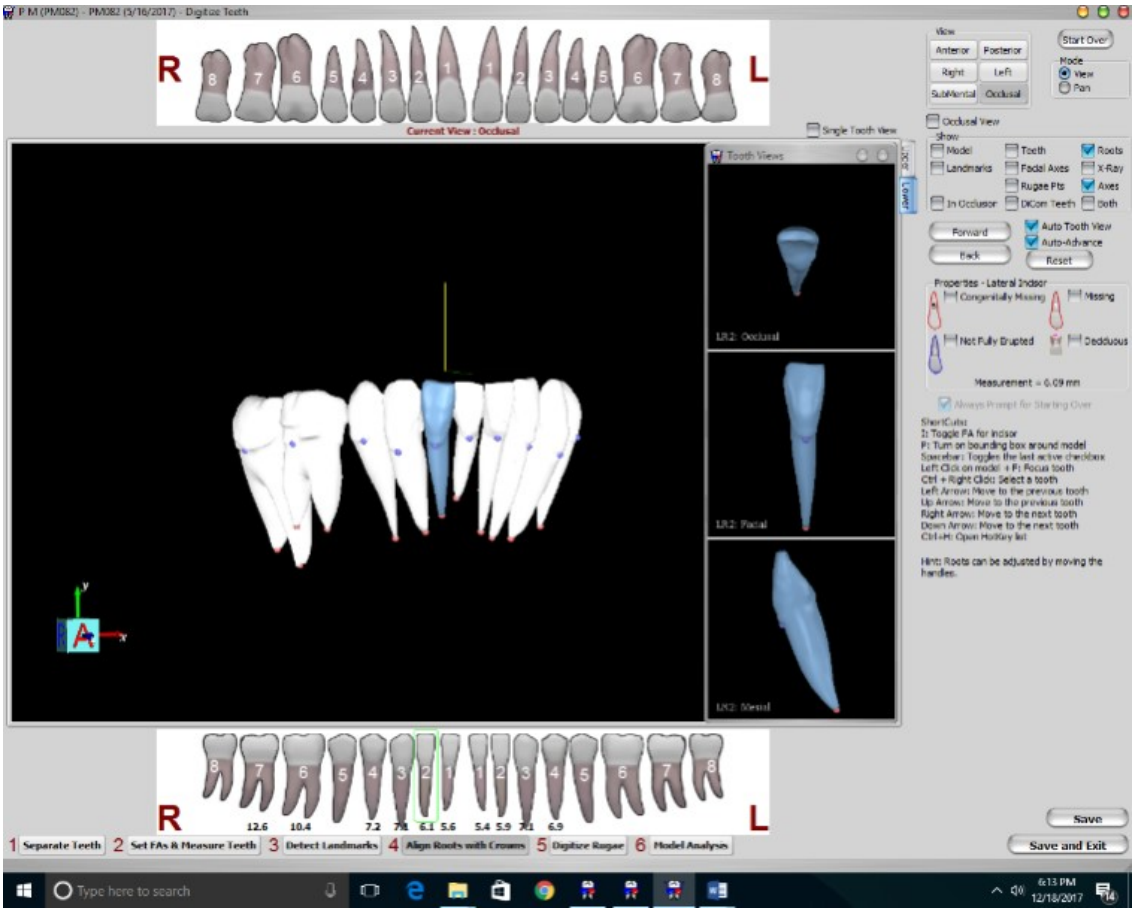

Figure 6. Root prediction and alignment of the roots with their corresponding crowns (082)

Figure 6. Root prediction and alignment of the roots with their corresponding crowns (Courtesy of Motion View Software LLC; printed with permission).

Their root predictions were also exported in STL file format (Figure 7).

Figure 7. Exported roots' predictions in STL file (Courtesy of Motion View Software LLC; printed with permission).

Models and root predictions with STL file format were loaded in the Viewbox software. The teeth extracted from the dry skulls were covered with a thin layer of white varnish in order to make them suitable for scanning.

The teeth were scanned in two stages in order to capture the whole surface: the first stage included scanning the crown and the cervical part of the root, extending as far apically as the retention base of the scanner would allow; at the second stage the tooth was turned over and the whole root was scanned together with part of the crown.

Three types of superimpositions were made so as to have all the teeth at a stable reference point for the successful estimation and comparison of their long axes:

The first superimposition aimed to construct one whole tooth model, out of the two separate parts obtained from the two scanning stages described above. The reference area for this superimposition was the common part of the two segments of each tooth (Figure 8).

Figure 8. Aunified tooth after the first superimposition of crown and root.

The second superimposition was conducted between each unified tooth model and the scanned plaster cast fabricated from the impressions taken from the dry human skulls. The reference area for this superimposition was the part of the crown visible on the casts. In most cases, the cemento-enamel junction was visible on the casts, so the whole crown was used, except for the contact areas to neighboring teeth (Figure9).

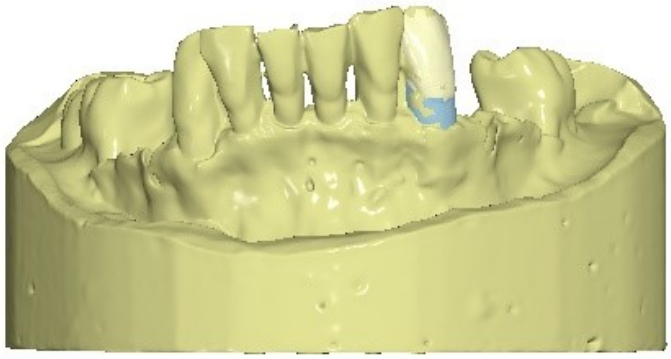

Figure 9. A superimposition of the tooth with the scanned plaster model.

The third superimposition was between the scanned plaster cast and the OrthoInsight prediction. More specifically, the OrthoInsight prediction included all the teeth of each jaw, joined together in one model. The crowns of both these predicted teeth and their casts were used as a reference point for the superimposition (Figure 10).

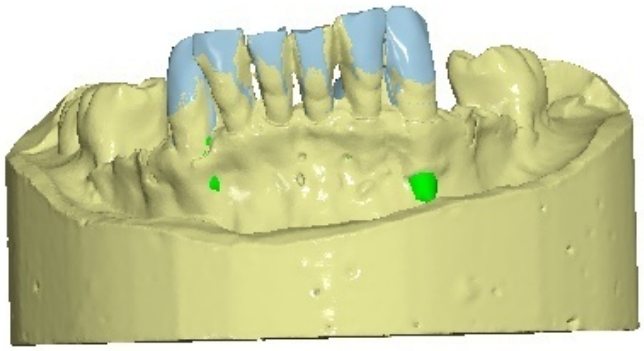

Figure 10. A superimposition of the scanned plaster cast and the OrthoInsight prediction.

The quality of all the superimpositions was assessed by the Root Mean Squared Distance (mm) (RMSD), computed as the square root of the average of the squared distances of the points of one of the surfaces to the closest point on the other surface (dHAL software, Viewbox, version 4.1.0.1 BETA).

Stage 2

The second part of the laboratory work consisted of landmarking the roots of both the real teeth and predicted ones to identify their long axes. Two different datasets were created for each tooth, one for the real tooth and the other for the prediction.

Each dataset was created by locating the root apex of every tooth and then choosing 3 random points on the surface of the root. By using these data, the dHAL Software was able to produce many points that were uniformly distributed on the root surface of every tooth and then each tooth long axis was computed as the best fit line to these points. Subsequently, the angle between the unified model of the actual tooth was estimated immediately automatically by the Dhal software after choosing one of them as a reference object (Figure 11).

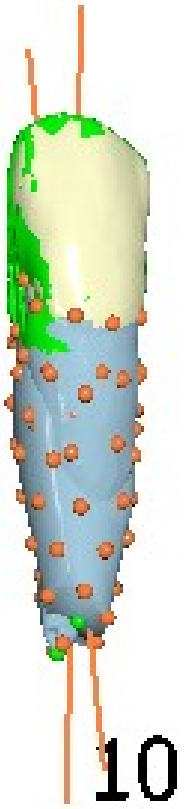

Figure 11. Estimation of the angulation between the long axes of the roots after the superimposition of the crown of the tooth with the crown of the prediction derived from the Ortho Insight Software.

6. Statistics

6.1. Sample Size Calculation

This study used dependent measurements and the hypothesis is based on the idea that

$$H_0: \mu_d = 0$$

Versus

$$H_1: \mu_d \neq 0$$

Where $\mu_d$is the mean difference in the population. The formula for determining the sample size to ensure that the accuracy of the test is acceptable:

$$n = \left(\frac{Z_{1-\alpha/2} + Z_{1-\beta}}{SE}\right)^2 * C$$

Where α is the selected level of significance and $Z_{1-\alpha/2}$ is the value from standard normal distribution holding 1- α/2 below, 1-β is the selected power and $Z_{1-\beta}$ is the value from standard normal distribution holding 1-β below it, C is the factor of proportionality of teeth selected per skull from expected total and SE is the effect size, defined as follows:

$$SE = \frac{\mu_d}{\delta_d}$$

Where $\mu_d$the mean difference is expected under the alternative hypothesis, H1, and δ_d is the standard of the difference in the outcome.

Based on the online site sample size calculator (powerandsamplesize.com), when

True mean, μ= 0°

Null Hypothesis mean, μ0 = 3°

Standard deviation, σ= 7°

Power, 1-β = 0,80°

α= 5%

The sample size, n is calculated 43.

In this research 55 anterior teeth were found.

6.2. Statistical Methods

Data were entered in an Excel file and SPSS for Windows (version 20.0, SPSS Inc., Chicago, Illinois, USA) was used for the representation of the data.

Diagrams and plots showing the quality of the overlaps and the results of the method's error testing were created.

After the calculation of the difference in the angulations between the long axis of the real tooth and the predicted axis, the median, the average, the quartiles and the standard deviation of the results were calculated and depicted in diagrams.

6.3. Method Error

In order to determine the degree of intra-examiner error of the measurements, fourteen teeth, one from each jaw of the sample, were randomly selected and the scanning was repeated by the author after an interval of one month. Overlapping between the crown and the root was again performed and a new RMSE was measured. Then the angle between the long axis of the rescanned tooth and the prediction was estimated and the difference, with their mean value were calculated as well.

The Bland Altman analysis was used to depict the validity of the statistical result. This was employed to describe agreement between the two quantitative measurements, one of the initial measurement and one after testing the method's error. This method is commonly used to quantify agreement between two quantitative measurements by constructing certain limits of agreement. These statistical limits are calculated by using the mean and the standard deviation of the differences between two measurements. To check the assumptions of normality of differences and other characteristics, a graphical approach is used. More specifically, the resulting graph is a scatter plot XY, in which the

Y axis shows the difference between the two paired measurements and the X axis represents the average of these measures. In other words, the difference of the two paired measurements is plotted against the mean of the two measurements(Bland and Altman, 1986).

7. Results

Assessing the quality of the superimpositions

The results of the method's error testing the crown-root and the tooth-cast superimpositions are depicted in two Bland-Altman plots which were drawn in order depict the agreement between the repeated measurements (Figures 12 and 13).

Regarding the overlap between the crown and the root, the dispersion of the values start from -0.006 to 0.010 indicating an acceptable reliability.

Regarding the overlap between the tooth and the cast, the dispersion of the values start from -0.040 to 0.057, also depicting a good quality of overlap.

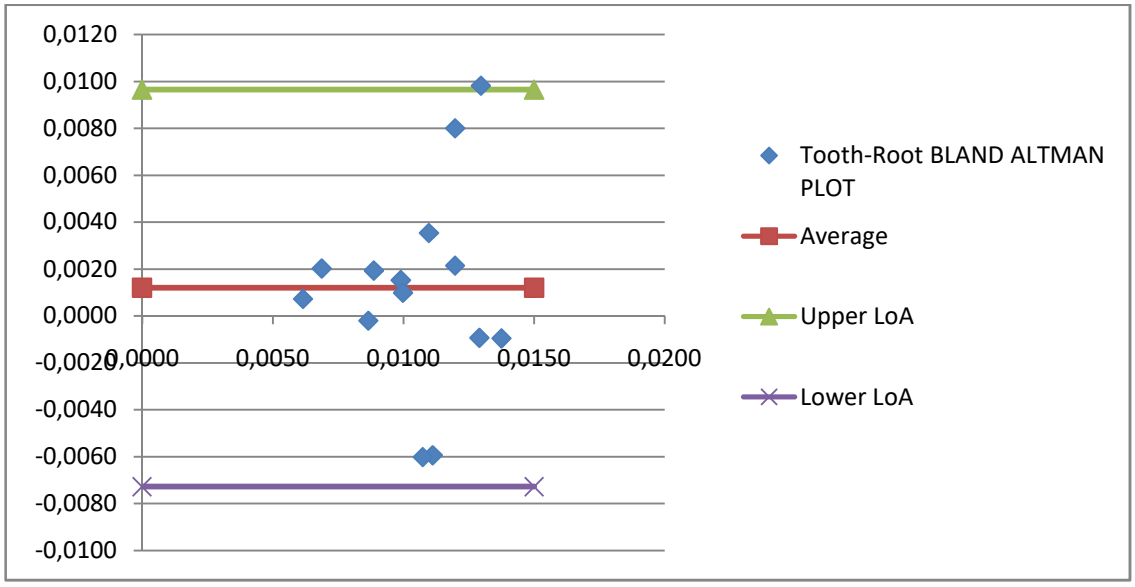

Figure 12. Tooth-Root Bland Altman Plot.

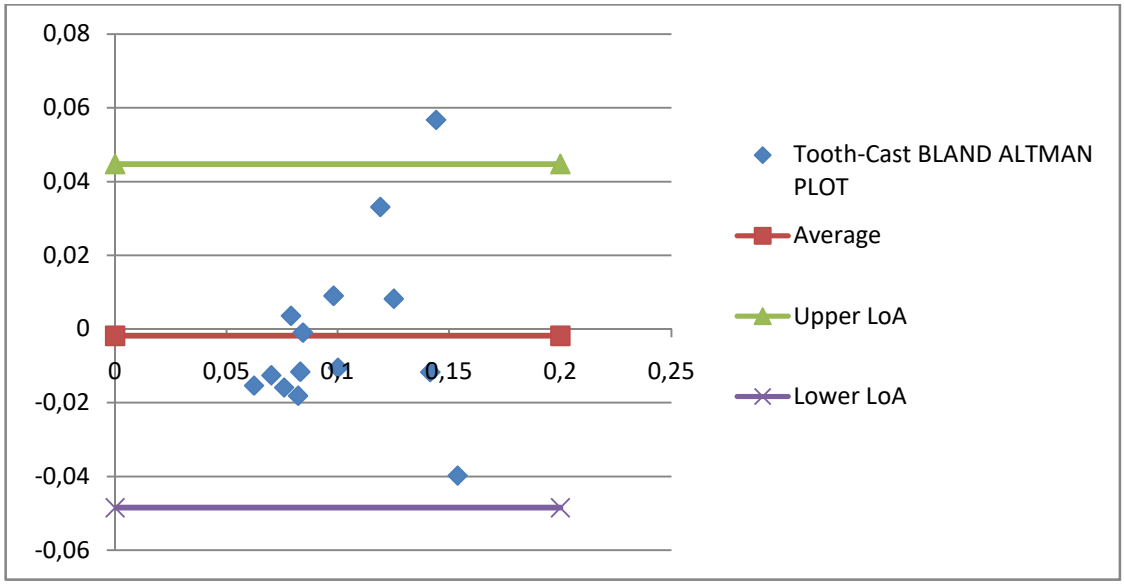

Figure 13. Tooth-Cast Bland Altman Plot.

The crown-root superimposition of the tooth segments was reliable and accurate, since the minimum value of the Root Mean Squared Distance (RMSD) was 0.005 mm, with the highest being 0.026 mm. The second superimposition that was conducted between each scanned copy of the 3D tooth included in the sample with the corresponding tooth of the scanned cast derived from the impressions taken from the dry human skulls, showed an RMSD ranging from 0.048 mm to 0.267mm indicating that the spread is wider compared to the overlap between the crown and the root. The last superimposition that was conducted was between the casts from the dry skulls and the prediction estimated by the Ortho Insight 3D laser scanners. The range from this comparison starts from 0.011 mm to 0.193 mm.

In conclusion, the best quality of the superimposition is achieved on the 1st overlap in which there are the minimum outliers compared to the other two, where the range is much wider, as shown in Figure 14.

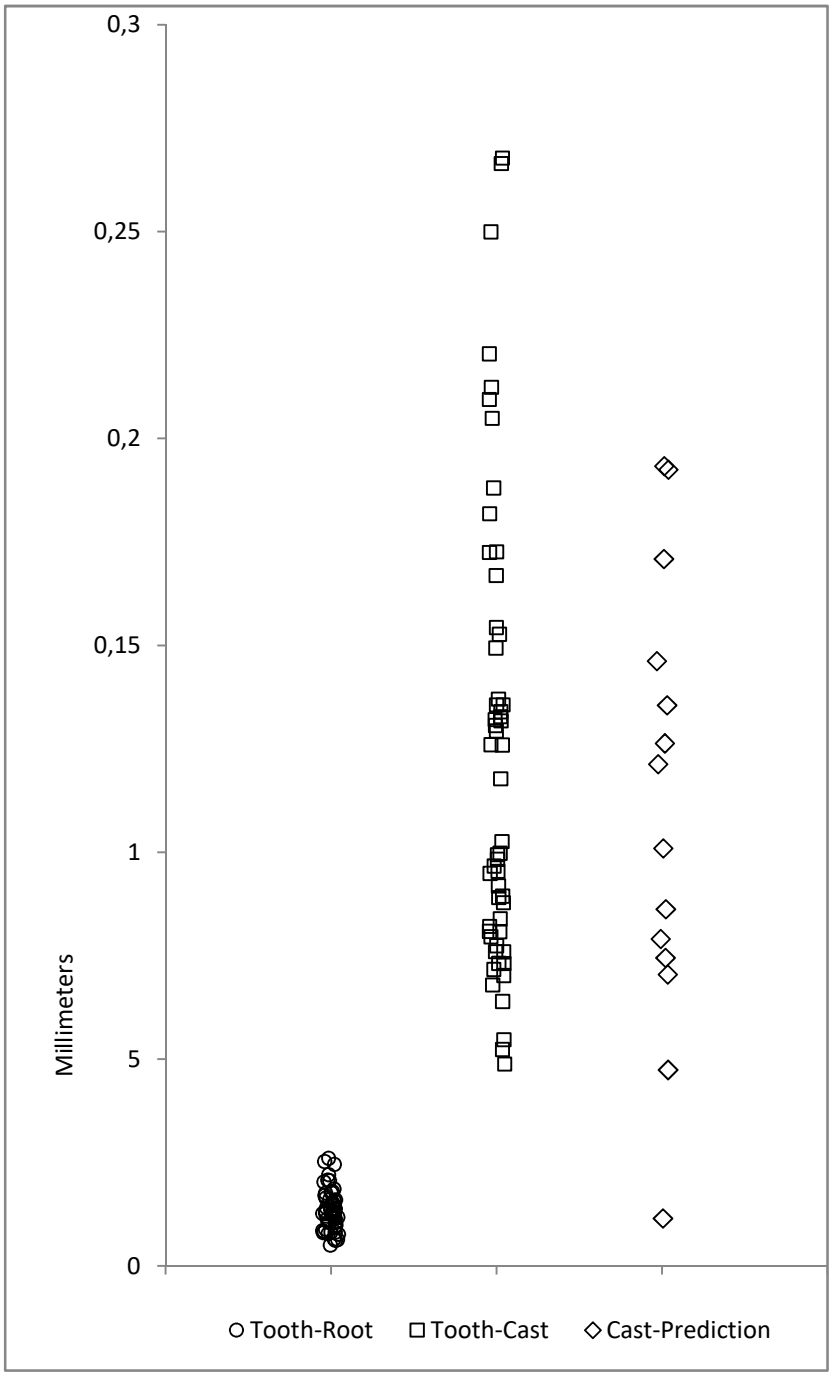

Figure 14. Superimpositions between tooth-root, tooth-cast and cast-prediction.

Assessing the results of the difference in angulation between the real and the predicted roots

The results of the method's error testing are shown in the Bland Altman plot of the Figure 15.

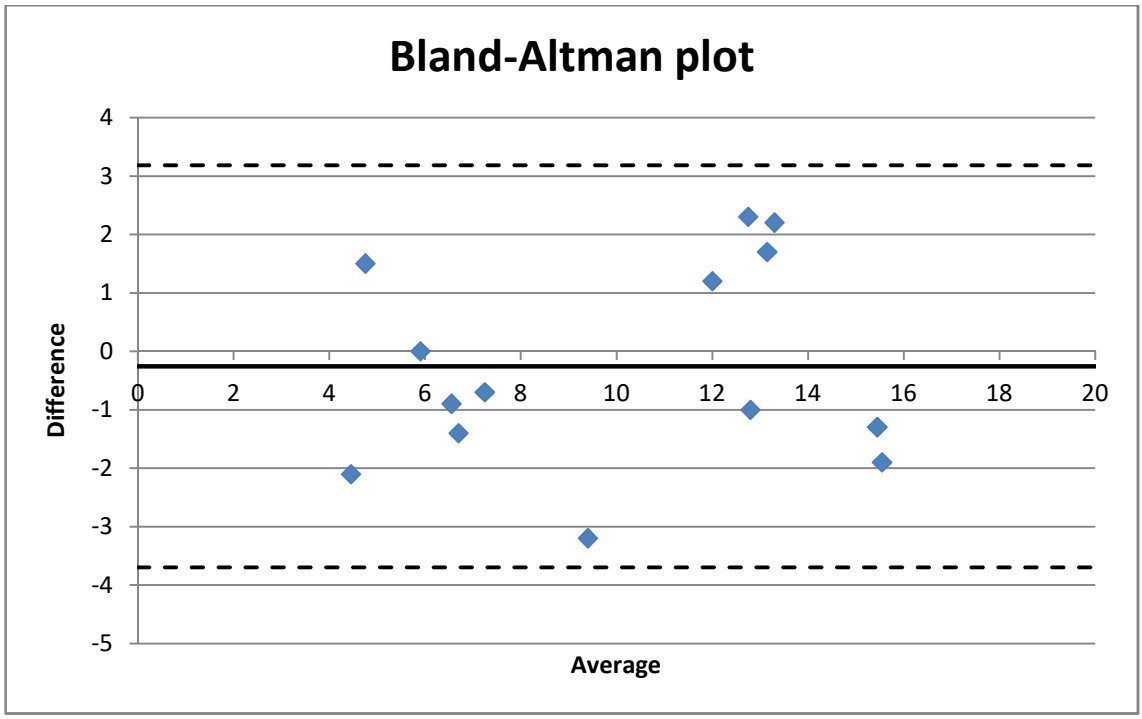

Figure 15. The error of the method for the difference in angulation between the real teeth and their predictions.

The mean value of the difference between repeated measurements was -0.2, the standard deviation was 1.75 and the 95% limits of agreement were from -3.69 to 3.18.

Figure 16 shows the angle formed between predicted and actual root inclination.

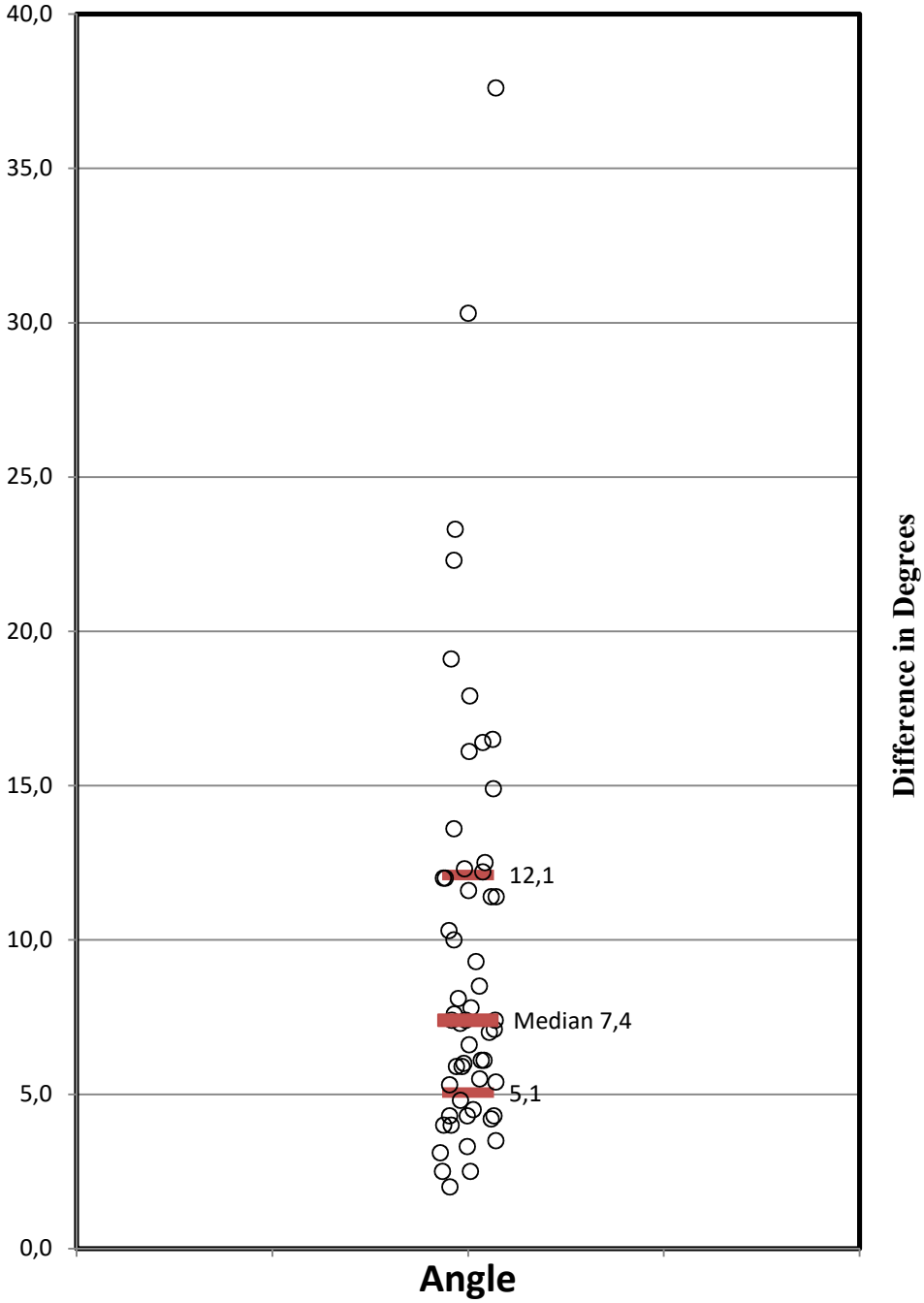

Figure 16. Difference in angulation between the real scanned teeth and their predictions.

The estimation that was calculated was between the long axis of the prediction of the tooth, and the long axis of the real scanned tooth.

The minimum value of these angles was 2.0 degrees and corresponded to a lower left lateral incisor of the sample, and the maximum one was 37.6 degrees and corresponded to an upper left lateral incisor.

The values for the median, 25% quartile, and 75% quartile were: 7.4, 5.1 and 12.1, respectively.

The mean value was 9.68 and the standard deviation was 6.96.

Also, Figure 17 shows a detailed graph indicating the difference in the angulation of the actual teeth and their corresponding predictions per tooth.

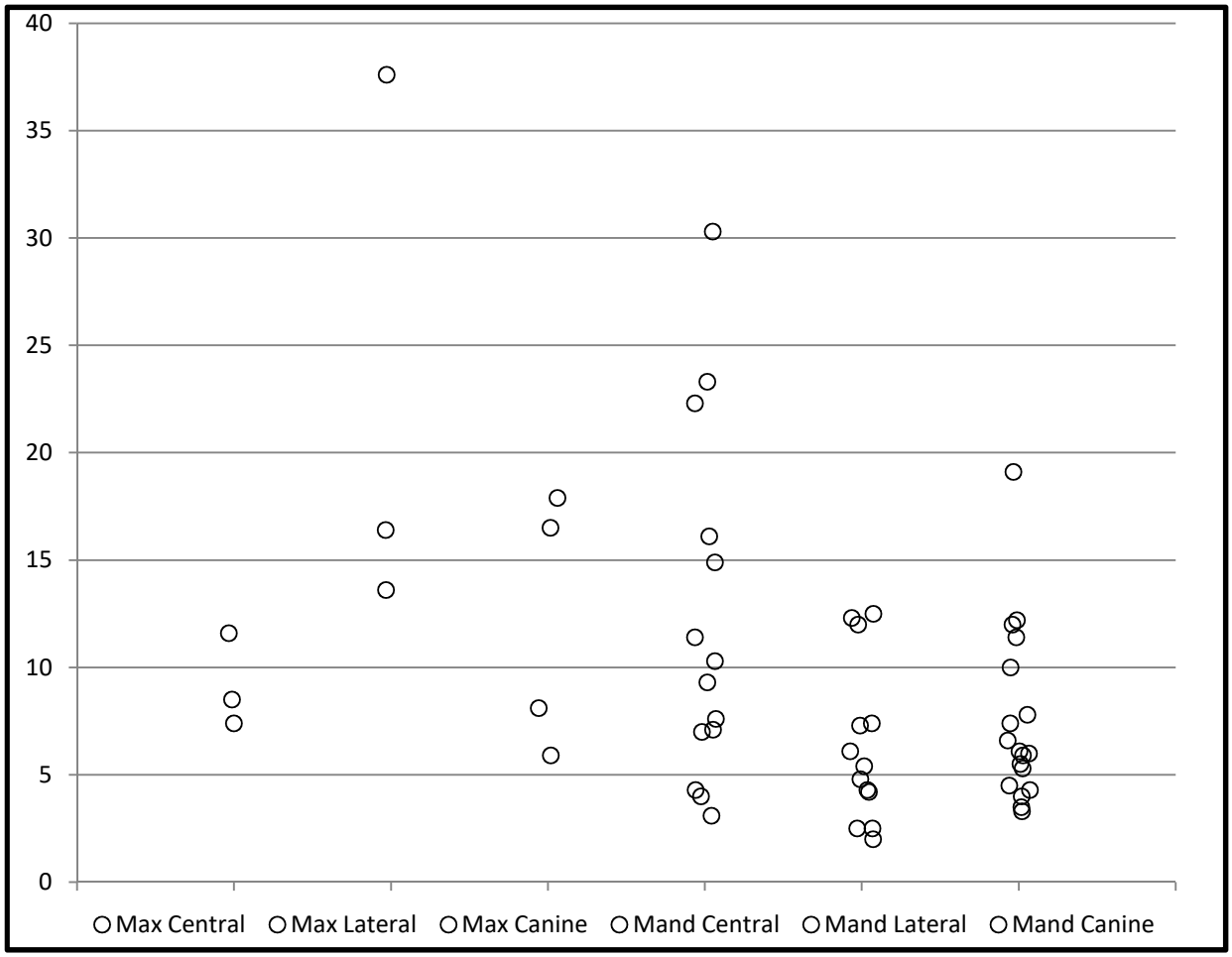

Figure 17. Detailed graph indicating the difference in the angulation of the real teeth and their corresponding predictions per tooth.

A test of normality indicates that the data were not normally distributed (Figure 18).

Tests of Normality

	Kolmogorov-Smirnov[a]			Shapiro-Wilk		
	Statistic	df	Sig.	Statistic	df	Sig.
VAR00001	,172	55	,000	,822	55	,000

a. Lilliefors Significance Correction

Figure 18. Normality test to assess the distribution of the teeth angles.

The results are also depicted on Table 5 which represents analytically their numerical angulation.

Table 5.Numerical representation of the difference in root angulation between the real tooth and the prediction.

Tooth	**Tooth Type**	**Jaw**	**Angle**
Tooth 13122	2	1	37,6
Tooth 05231	1	2	30,3
Tooth 13113	3	1	17,9
Tooth 12243	3	2	11,4
Tooth 05241	1	2	23,3
Tooth 03241	1	2	22,3
Tooth 01233	3	2	6,6
Tooth 06233	3	2	19,1
Tooth 07112	2	1	16,4
Tooth 09241	1	2	16,1
Tooth 07122	2	1	13,6
Tooth 08241	1	2	7,1

Tooth 03233	3	2	10
Tooth 03232	2	2	12,3
Tooth 13123	3	1	16,5
Tooth 04241	1	2	10,3
Tooth 05243	3	2	7,4
Tooth 04231	1	2	11,4
Tooth 04232	2	2	12
Tooth 03231	1	2	14,9
Tooth 03242	2	2	4,2
Tooth 14111	1	1	11,6
Tooth 05232	2	2	12,5
Tooth 10243	3	2	12,2
Tooth 05242	2	2	7,4
Tooth 07111	1	1	7,4
Tooth 09233	3	2	7,8
Tooth 09242	2	2	7,3
Tooth 05233	3	2	12
Tooth 06231	1	2	7,6
Tooth 07113	3	1	8,1
Tooth 02241	1	2	7
Tooth 04242	2	2	5,4
Tooth 06241	1	2	4,3
Tooth 04243	3	2	5,9
Tooth 10241	1	2	3,1
Tooth 09243	3	2	6,1
Tooth 10242	2	2	2,5
Tooth 08243	3	2	4
Tooth 08231	1	2	4

Tooth 08242	2	2	4,3
Tooth 09232	2	2	6,1
Tooth 06243	3	2	3,3
Tooth 07123	3	1	5,9
Tooth 10231	1	2	9,3
Tooth 07121	1	1	8,5
Tooth 08233	3	2	4,3
Tooth 02232	2	2	4,8
Tooth 08232	2	2	2
Tooth 02242	2	2	2,5
Tooth 02243	3	2	4,5
Tooth 03243	3	2	6
Tooth 02233	3	2	3,5
Tooth 04233	3	2	5,3
Tooth 11233	3	2	5,5

8. Discussion

Many reports indicate a rapid growth in the use of digital models in the field of dentistry (Keim et al., 2008, Martin et al., 2015). These studies support that, in general, digital softwares are able to reproduce dental structures with a high degree of accuracy (Hirogaki et al., 2001).

The present investigation attempted to evaluate the validity of the root inclination prediction capability of digital models derived from a commercially available software (Ortho Insight 3D scanner software)by comparison with real teeth from dry human skulls.

There is only one relevant previous study that evaluated root inclination predictions derived from digital models using the same software with this investigation, but compared with root images derived from CBCT images (Dastoori, 2016). This study showed a large range of discrepancies in the angle between the images derived from digital models and CBCT data, reaching almost 40 degrees in extreme cases (upper left canine). The canines showed the worst discrepancies, followed by the lower lateral incisors. The upper central incisors exhibit the best comparisons, although the maximum difference in angle exceeds 20 degrees (but the median was only around 8 degrees).

In this investigation,26 teeth were above the value of the median (7.4) with three teeth(two lower central incisors and one upper lateral incisor) displaying extreme values of 23.3, 30.3 and 37.3 degrees of difference in angulation. The remaining 28 teeth have a value below the median, and the three minimum values are found in cases of lower lateral incisors, with the values of 2 and 2.5 degrees.

According to Mayor's classification of root parallelism, errors of 10 degrees and more in estimating teeth mesio-distal or labio-lingual inclination should be considered as clinically significant, since the parallelism is characterized as poor (Mayor, 1982).

Extreme variability in the prediction of root inclination could be a serious issue and cannot be an acceptable performance of a software in the clinical environment. On the other hand, if the root inclination can be accurately predicted by digital means the quality of orthodontic therapy can be greatly benefitted. Biomechanical adjustments of fixed appliances, proper attachment placement in clear aligner treatments and temporary anchorage devices' placement are a few examples of the potential positive outcomes of an accurate root inclination prediction by scanning the crowns of the teeth. Additional information regarding the resorption of the roots or the angulation of the apex (e.g. dilacerated roots), comprises a significant advantage in the treatment planning in orthodontics.

The present study has inherent limitations due to the relatively small number of the teeth used to test the software and the restriction of the sample to the anterior area of the dental arches. With regard to the later and following a preliminary visual evaluation of the digital models, anterior teeth are simpler in terms of the morphology of both their crowns and roots. The assessment of root inclination differences between images of the digital models and data from the real teeth indicates that other important morphological features, such as root length, volume, shape, were not included.

Furthermore, the data from the results of this investigation do not indicate the direction of the angulation error, i.e. whether it was in mesio-distal or labio-lingual direction, while in certain cases overlapping of the roots of the adjacent teeth was taking place. Another reason for the outliers found may be the type of the material used for the impressions, since alginate misrepresents the exact dimensions of the teeth and can produce slightly altered dimensions for the real teeth.

Additionally, after scanning the plaster study casts, it was revealed that the interdental areas were not depicted accurately and, as a result, during the superimposition of the real teeth with the plaster casts, the degree of accuracy was limited. This discovery is of great significance for the outcomes of the study.

Finally, the thickness of the varnish used to cover the teeth to enhance the quality of the scanned images may have affected the results of the superimposition, as thicker layers might have affected the quality of the superimposition between the teeth and the scanned casts.

On the other hand, the commercially available software used in this investigation has received excellent reviews regarding use in providing dental arch measurements as well as in performing space analyses, tooth size discrepancy evaluation and other orthodontic applications based on landmarks derived from tooth crown morphology (Dastoori, 2016). The sensitivity of the methodology employed in superimposing teeth crowns of real teeth with digital models thus forms one of the limitations of this project. Root morphology imaging prediction is not a specific function this software is designed to provide, and this study confirms its limitation in routine clinical applications when used alone. However, the simulation of root morphology based on scanning plaster dental models, or dental impressions is an initial further step which would prove very advantageous in the future, if the accuracy of the prediction can be significantly improved.

The clinical application of this investigation has a major influence in eliminating the use of CBCT radiography and the exposure of the patient in other types of x-rays, as well in certain companies that are using a combination of 3D scanning and x-rays as basic tools for the conduction of the treatment planning. Such companies are SureSmile® (OraMetrix, Inc. Richardson, TX, USA) that produces customised arch-wires ideal for surgical cases and finishing, Incognito™ (3M, St. Paul, MN, USA), which is the pioneer in the customization of lingual fixed orthodontic appliances and arch-wires, Insignia™ (ORMCO, Orange, CA, USA), which are customised buccal fixed orthodontic appliances (brackets), in house aligner fabrication with the advancement of 3D printers, software etc and could set the orthodontist independent from aligner manufacturers.

Providing the application of this software prediction to such companies, would eliminate the use of the x-rays as diagnostic tools.

It is evident that, at the present time, these predictions cannot be considered accurate and reliable unless they are correlated with radiographic images. If this kind of software could be improved to predict all the required criteria available for evaluation in a radiograph, without the need to expose the patient to additional radiation, it would provide significant clinical benefits.

9. Conclusions

This investigation was carried out to test the hypothesis that there are differences in predicted anterior teeth root inclination characteristics generated by commercially available 3D laser scanner software and the inclination characteristics derived from teeth removed from dry human skulls. The research hypothesis was verified because significantly different anterior teeth root inclinations between the two images have been clearly demonstrated.

The results of the study lead to the following conclusions:

- A median value for the angle between true root position derived from real teeth and estimated position ranging from 2 to 37.6 degrees with a mean value of 9.7 degrees was found.
- The degree of error is higher for mandibular central incisors and maxillary lateral incisors, and lower for maxillary central incisors and mandibular lateral incisors.
- Visual observation of the cases proved that the software frequently estimates angulations that create overlapping of adjacent roots, a clinically impossible situation unless there is extensive root resorption or root morphology variation.
- Further investigations and improvements of the software are needed before it can be considered effective for routine clinical use.

10. References

Akyalcin S. Are digital models replacing plaster casts? Dentistry. 2011;1:e102.

Akyalcin S, Dyer DJ, English JD, Sar C. Comparison of 3-dimensional dental models from different sources: diagnostic accuracy and surface registration analysis. Am J OrthodDentofacialOrthop. 2013;144:831-7.

Alamadi E, Alhazmi H, Hansen K, Lundgren T, Naoumova J. A comparative study of cone beam computed tomography and conventional radiography in diagnosing the extent of root resorptions. Prog Orthod. 2017;20:18-37.

Anh JW, Park JM, Chun YS, Kim M, Kim M. A comparison of the precision of three-dimensional images acquired by 2 digital intraoral scanners: effects of tooth irregularity and scanning direction. Korean J Orthod. 2016;46:3-12.

Armstrong D, Kharbanda OP, Petocz P, Darendeliler MA. Root resorption after orthodontic treatment. Aust Orthod J. 2006;22:153-60.

Biggerstaff RH, Phillips JR. A quantitative comparison of paralleling long-cone and bisection-of-angle periapical radiography. Oral Surg Oral Med Oral Pathol. 1976;62:673–7.

Black V. Descriptive anatomy of the human teeth. Philadelphia: S S White, 1902.

Bland JM, Altman DG. Statistical methods for assessing agreement between two methods of clinical measurement. Lancet. 1986;8:307-10.

Bushberg JT, Seibert JA, Leidholdt EM, Boone JM. The essential physics of medical imaging. Baltimore: Lippincott Williams and Wilkins, 2012.

Carter L, Farman AG, Geist J. American Academy of Oral and Maxillofacial Radiology executive opinion statement on performing and interpreting diagnostic cone beam

computed tomography. Oral Surg Oral Med Oral Pathol Oral Radiol Endod. 2008;106:561–2.

Dahlberg G. Statistical Methods for Medical and Biological Students. Br Med J 1940;14:358-9.

Dastoori M. Root inclination prediction derived from digital models: A comparative study of plaster study casts and CBCT images. Master of Science in Orthodontics. Dubai: Hamdan Bin Mohammed College of Dental Medicine, Mohammed Bin Rashid University of Medicine and Health Sciences, 2016.

Farman AG. Panoramic Radiology: Seminars on Maxillofacial Imaging and Interpretation. Berlin, Springer, 2007.

Fleming PS, Marinho V, Johal A. Orthodontic measurements on digital study models compared with plaster models: a systematic review. Orthod Craniofac Res. 2011;14:1-16.

Flores-Mir C, Rosenblatt MR, Major PW, Carey JP, Heo G. Measurement accuracy and reliability of tooth length on conventional and CBCT reconstructed panoramic radiographs. Dental Press J Orthod. 2014;19:45-53.

Garino F, Garino B. From digital casts to digiral occlusal set up: An enhanced diagnostic tool. World J Orthod. 2003;4:162-6.

Grünheid T, McCarthy SD, Larson BE. Clinical use of a direct chairside oral scanner: an assessment of accuracy, time, and patient acceptance. Am J Orthod Dentofacial Orthop. 2014;146:673-82.

Halazonetis DJ. Cone-beam computed tomography is not the imaging technique ofchoice for comprehensive orthodontic assessment. Am J Orthod Dentofacial Orthop. 2012;141:403, 405, 407.

Han UK, Vig KW, Weintraub JA, Vig PS, Kowalski CJ. Consistency of orthodontic treatment decisions relative to diagnostic records. Am J Orthod Dentofac Orthop. 1991;100:212-9.

Hirogaki Y, Sohmura T, Satoh H, Takahashi J, Takada K. Complete 3-D reconstruction of dental case shape using perceptual grouping. IEEE Trans Med Imaging. 2001;20:1093-101.

Iannucci J, Howerton J. Dental Radiography: Principles and Techniques. St Louis, Saunders, 2006.

Idiyatullin D, Corum C, Moeller S. Dental magnetic resonance imaging: making the invisible visible. J Endod. 2011;37:745–52.

Isaacson KG, Thom AR, Atack NE, Horner K, Whaites E. Guidelines for the Use of Radiographs in Clinical Orthodontics. London, British Orthodontic Society, 2015.

Jacob HB, Wyatt GD, Buschang PH. Reliability and validity of intraoral and extraoral scanners. Prog Orthod. 2015;16:38.

Kravitz ND, Groth C, Jones PE, Graham JW, Redmond WR. Intraoral digital scanners. J Clin Orthod. 2014;48:337-47.

Keating AP, Knox J, Bibb R, Zhurov AI. A comparison of plaster, digital and reconstructed study model accuracy. J Orthod. 2008;35:191-201.

Keim RG, Gottlieb EL, Nelson AH, Vogels DS. Study of orthodontic diagnosis and treatment procedure, part 1: Results and trends. J Clin Orthod. 2008;42:625-40.

Koussoulakou D, Margaritis L, Koussoulakos S. A curriculum vitae of teeth: Evolution, generation, regeneration. Int J Biol Sci. 2009;5:226-43.

Kumar M, Shanavas M, Sidappa A, Kiran M. Cone beam computed tomography - know its secrets. J Int Oral Health. 2015;7:64-8.

Langland O, Langlais R, Preece J. Principles of Dental Imaging. Alphen aan den Rijn, Wolters Kluwer, 2002.

Lestrel PE. Some approches toward the mathematical modeling of the craniofacial complex. J Craniofac Genet Dev Biol. 1989;9:77-91.

Liebgott B. The Anatomical Basis of Dentistry. St. Louis, Mosby, 2001.

Leifert MF, Leifert MM, Efstratiadis SS, Cangialosi TJ. Comparison of space analysis evaluation with digital models and plaster dental casts. Am J Orthod Dentofacial Orthop. 2009;136:16.e1-4.

Mandelli F, Gherlone E, Gastaldi G, Ferrari M. Evaluation of the accuracy of extraoral laboratory scanners with a single-tooth abutment model: A 3D analysis. J Prosthodont Res. 2017;61:363-70.

Martin CB, Chalmers EV, McIntyre GT, Cochrane H, Mossey PA. Orthodontic scanners: what is available? J Orthod. 2015;42:136-43.

Matalova E, Tucker AS, Sharpe PT. Death in the life of a tooth. J Dent Res. 2004;83:11-6.

Mayoral G. Treatment results with light wires studied by panoramic radiography. Am J Orthod. 1982;81:489-97.

Merrett SJ, Drage NA, Durning P. Cone beam computed tomography:
a useful tool in orthodontic diagnosis and treatment planning. J Orthod. 2009;36:202-10.

Melsen B, Agerbæk N, Markenstam G. Intrusion of incisors in adult patients with marginal bone loss. Am J Orthod Dentofac Orthop. 1989;96:232-41.

Nasiopoulos AT, Athanasiou AE, Papadopoulos MA, Kolokithas G, Ioannidou I. Premolar root changes following treatment with the banded Herbst appliance. J Orofac Orthop. 2006;67:261-71

Niraj LK, Patthi B, Singla A, Gupta R, Ali I, Dhama K, Kumar JK, Prasad M. MRI in Dentistry- A future towards radiation free imaging – Systematic review. J Clin Diagn Res. 2016;10:ZE14-ZE19.

Nelson S, Ash M. Wheeler's Dental Anatomy, Physiology, and Occlusion. New York, Elsevier, 2010.

Paatero YV. The use of a mobile source of light in radiography. Acta Radiol. 1948;29:221-7.

Peluso M, Josell S, Levine S, Lorei B. Digital models: An introduction. Semin Orthod. 2004;10:226-38.

www.orthodonticproductsonline.com

www.planmeca.com

Porter JL. Comparison of intraoral and extraoral scanners on the accuracy of digital model articulation. Richmond, Virginia Commonwealth University, 2017. http://scholarscompass.vcu.edu/etd/4881

Qu XM1, Li G, Ludlow JB, Zhang ZY, Ma XC. Effective radiation dose of ProMax 3D conebeam computerized tomography scanner with different dental protocols. Oral Surg Oral Med Oral Pathol Oral Radiol Endod. 2010;110:770-6.

Radiation Protection Series Publication, European Commission. Brussels, European Commission, 2012. https://ec.europa.eu/energy/en/radiation-protection-publications

Read DW, Lestrel PE. A comment upon uses of homologous-point measures in systematic: a reply to Brookstein et al. Syst Zool 1986;35:241-53.

Rheude B, Sadowsky PL, Ferriera A, Jacobson A. An evaluation of the use of digital study models in orthodontic diagnosis and treatment planning. Angle Orthod. 2005;75:300-4.

Ross JR, Matava MJ. Tattoo-Induced Skin “Burn” DuringMagnetic Resonance Imaging in aProfessional Football Player:A Case Report. Sports Health 2011;3:431-4.

Rossini G, Parrini S, Castroflorio T, Deregibus A, Debernardi CL. Diagnostic accuracy and measurement sensitivity of digital models for orthodontic purposes: A systematic review. Am J Orthod Dentofacial Orthop. 2016;149:161-70.

Rushton VE, Rout J: Panoramic Radiology. London; Quintessence Publishing Co, 2006.

Scarfe WC, Li Z, Aboelmaaty W, Scott SA, Farman AG. Maxillofacial cone beam computed tomography: essence, elements and steps to interpretation. Aust Dent J. 2012;57:46–60.

Scheid R, Weiss G. Woelfel’s Dental Anatomy. Alphen aan den Rijn; Wolters Kluwer, 2017.

Scott J, Symons N. Introduction to Dental Anatomy. Harlow, Longman, 1977.

Sinaloglu A, Helvacioglu-Yigit D, Mutlu I. Use of cone-beam computed tomography and three-dimensional modeling for assessment of anomalous pulp canal configuration: a case report. Restor Dent Endod. 2015;40:161-5.

Stewart MB. Dental models in 3D. Orthod Prod. 2001;21-4.

Sherrard JF, Rossouw PE, Benson BW, Carrillo R, Buschang PH. Accuracy and reliability of tooth and root lengths measured on cone-beam computedtomographs. Am J Orthod Dentofacial Orthop. 2010;137(4 Suppl):S100-8.

Thesleff I, Vaahtokari A, Partanen AM. Regulation of organogenesis. Common molecular mechanisms regulating the development of teeth and other organs. Int J Dev Biol. 1995;39:35-50.

Thiruvenkatachari B, Al-Abdallah M, Akram NC, Sandler J, O'Brien K. Measuring 3-dimensional tooth movement with a 3-dimensional surface laser scanner. Am J Orthod Dentofacial Orthop. 2009;135:480-5.

Tutton LM, Goddard PR: MRI of the teeth. Br J Radiol. 2002;75:552–62.

Tymofiyeva O, Proff PC, Rottner K, Düring M, Jakob PM, Richter EJ. Diagnosis of dental abnormalities in children using 3-dimensional magnetic resonance imaging. J Oral Maxillofac Surg. 2013;71:1159-69.

Wesemann C, Muallah J, Mah J, Bumann A. Accuracy and efficiency of full-arch digitalization and 3D printing: Acomparison between desktop model scanners, an intraoral scanner, a CBCT model scan, and stereolithographic 3Dprinting. Quintessence Int. 2017;48:41-50.

Westbrook C, Roth CK, Talbot J. MRI in practice. Oxford, Wiley-Blackwell, 2011.

Weishaupt D, Köchli V, Marincek B. How Does MRI Work? An Introduction to the Physics and Function of Magnetic Resonance Imaging. Berlin, Springer, 2008.

White S, Pharoah M. Oral Radiology: Principles and Interpretation. St. Louis, MosbyElsevier, 2009.

Yau HT, Yang TJ, Chen YC. Tooth model reconstruction based upon data fusion for orthodontic treatment simulation. Comput Biol Med. 2014;48:8-16.

Zhang ZL, Cheng JG, Li G, Zhang JZ, Zhang ZY, Ma XC. Measurement accuracy of temporomandibular joint space in Promax 3-dimensional cone-beam computerized tomography images. Oral Surg Oral Med Oral Pathol Oral Radiol. 2012;114:112-7.